Primljen / Received: 5.12.2017.
Ispravljen / Corrected: 12.3.2018.
Prihvaćen / Accepted: 18.4.2018.
Dostupno online / Available online: 10.7.2018.

Seismic upgrading of isolated bridges with SF-ED devices:Shaking table tests on large-scale model

Authors:

[1]Assist.Prof. **Jelena Ristić**, PhD. CE
jelena.ristik@live.com

[2]Assoc.Prof. **Misin Misini**, PhD. CE
misin.misini@uni-pr.edu

[3]Prof. **Danilo Ristić**, PhD. CE
danilo.ristic@gmail.com

[2]**Zijadin Guri**, MsC. CE
guri.zijadin@gmail.com

[4]**Nebi Pllana**, PhD. CE
npllana@ipe-proing.com

[1]FON University, Faculty of Architecture, Skopje, Macedonia
[2]University of Prishtina, Faculty of Civil Engineering and Architecture, Prishtina, Kosovo
[3]Institute of Earthquake Engineering and Engineering Seismology (IZIIS), Skopje, Macedonia
[4]IPE-Proing, Prishtina, Kosovo

Original scientific paper

Jelena Ristić, Misin Misini, Danilo Ristić, Zijadin Guri, Nebi Pllana

Seismic upgrading of isolated bridges with SF-ED devices:Shaking table tests on large-scale model

Results of original experimental research, obtained during shaking table tests on a large-scale bridge model equipped with an advanced seismic protection system type USI-SF, are presented in the paper. The installed basic seismic isolation system is created by applying novel double spherical rolling seismic bearing (DSRSB) devices, while qualitative upgrading of seismic performances is made using the installed advanced multi-directional space flange energy dissipation (SF-ED) devices. Research results show that significant qualitative improvement of seismic performances of isolated road bridges can be achieved using DSRSB and SF-ED devices.

Key words:
bridge, seismic isolation, shaking table, ductility, energy dissipation, seismic safety

Izvorni znanstveni rad

Jelena Ristić, Misin Misini, Danilo Ristić, Zijadin Guri, Nebi Pllana

Seizmičko poboljšanje izoliranih mostova pomoću uređaja SF-ED: Ispitivanje modela u velikom mjerilu na potresnom stolu

U radu su prikazani rezultati originalnog eksperimentalnog istraživanja na potresnom stolu modela mosta u velikom mjerilu koji je opremljen naprednim sustavom seizmičke zaštite tipa USI-SF. Instalirani osnovni sustav seizmičke izolacije izveden je primjenom novih dvojnih kružnih kotrljajućih seizmičkih ležajeva (DSRSB), a kvalitativno poboljšanje seizmičkih karakteristika provedeno je pomoću instaliranih naprednih višesmjernih prostornih pojasnih uređaja za rasap energije (SF-ED). Rezultati istraživanja pokazuju da se primjenom uređaja DSRSB i SF-ED mogu postići značajna kvalitativna poboljšanja seizmičkih karakteristika izoliranih cestovnih mostova.

Ključne riječi:
most, seizmička izolacija, potresni stol, duktilnost, rasap energije, seizmička sigurnost

Wissenschaftlicher Originalbeitrag

Jelena Ristić, Misin Misini, Danilo Ristić, Zijadin Guri, Nebi Pllana

Seismische Verbesserung der mit dem Gerät SF-ED isolierten Brücken: Untersuchung des Modells in großem Maßstab auf dem Erdbebentisch

In der Abhandlung werden die Ergebnisse der ursprünglichen experimentellen Untersuchung des Brückenmodells in großem Maßstab auf dem Erdbebentisch dargelegt, das mit einem fortschrittlichen System des seismischen Schutzes des Typs USI-SF ausgestattet ist. Das installierte seismische Basisisoliersystem wurde durch Verwendung neuer doppelter kreisrunder rollender seismischer Lager ausgeführt (DSRSB), und die qualitative Verbesserung der seismischen Eigenschaften wurde mithilfe der installierten fortschrittlichen multidirektionalen räumlichen Energieverteilungsvorrichtung (SF-ED) durchgeführt. Die Ergebnisse der Untersuchungen zeigen, dass man durch die Verwendung der Geräte DSRSB und SF-ED eine Verbesserung der seismischen Eigenschaften der isolierten Straßenbrücken erreichen kann.

Schlüsselwörter:
Brücke, seismische Isolierung, Duktilität, Energieverteilung, seismische Sicherheit

1. Introduction

The most important research in the field of seismic isolation of bridge structures was originally carried out in the most renowned research centres in Japan, USA, Italy, New Zealand, etc. In recent times, investigations in this specific field have been intensified and extended so as to include many other countries worldwide. Due to great diversity of innovative ideas, the research performed so far has most frequently been strictly focused on the development of specific individual devices, such as:

- rubber seismic bearings
- sliding seismic bearings
- rolling seismic bearings
- devices for limitation of displacements
- purpose-oriented analytical research
- purpose-oriented experimental research
- research for introducing seismic isolation in practice.

A thorough and detailed insight into achievements made so far in the world in this specific field is given in comprehensive reviews published by a number of authors, [1, 2]. Specific characteristics of hysteretic behaviour of common rubber and lead-rubber seismic bearings are presented in [3, 4]. Specific behaviour of sliding seismic bearings [5-7], and of the recently developed simple pendulum seismic bearings [8, 9], has been comprehensively studied, experimentally validated, [10, 11], and introduced in current practice. The concept of applying the proposed additional devices for seismic energy dissipation, [12-14, 20-22], along with some devices for limitation of large displacements, has been introduced. Lately, the developments in this innovative earthquake engineering field have been intensified with complementary studies of various specific related phenomena, including the pounding effect [15], axial behaviour of elastomeric isolators [16], semi-active dampers [17], as well as with studies devoted to qualitative upgrading of present technologies. Seismic design regulations for seismically isolated bridges have been gradually introduced and are continuously upgraded [18] and implemented in many countries located in seismically active regions [19]. In their conclusions, most authors provide recommendations on the need to undertake further studies in this scientific field, including advanced ideas for upgrading the existing isolation systems. Catastrophic seismic damage to traditional bridges, observed during recent strong earthquakes, is usually due to insufficient resistance of bridge bearings, inappropriate design of super-and/or substructure systems, and to inadequate design of foundations with regard to actual local soil conditions. Commonly, the bridge substructure deforms, settles, suffers permanent displacements and large cracks, or is overturned. The superstructure is commonly displaced, which is accompanied by the opening of large cracks, or it fails completely. Even modern bridges experience very serious damage in case of unexpectedly strong earthquakes. Strict standards for safety and functioning are nowadays applied for both new and existing bridge structures. The following typical design shortcomings have so far been observed in practice:

- actual design of seismically isolated structures has been done from case to case, without defining all risk factors important for developing safe technical solutions
- some additional energy dissipation elements have been designed separately for longitudinal and separately for transverse directions, which is physically inappropriate since the earthquake generally acts in all directions. Therefore, there is a pressing need to introduce advanced devices that will protect the structure against earthquake effects from any direction
- in some cases, extensive damage or total failure can occur because of the lack of safe technological solutions that could limit very large displacements caused by the strongest earthquakes.

This research project was initiated in response to the existing problems regarding catastrophic impacts on bridge structures due to strong earthquakes, which experience collapse even in the most developed countries worldwide. The research presented in this paper actually resulted in the development of an original advanced and experimentally verified option of an upgraded seismically isolated system with space flange devices, USI-SF system, representing qualitative contribution to solving complex problems related to advanced design of seismically resistant bridge structures with controlled level of seismic damage and undisturbed functioning in the case of very strong future earthquakes.

2. Background of USI-SF seismic protection system for bridges

2.1. Clarification of actual needs for technological advancement

To provide for an undisturbed functioning of highway bridges in seismic regions during their long service life (200 years or more), it is necessary to develop an upgraded seismic isolation system that would be capable of avoiding destructive effects of repeated strong earthquakes. Severe destructive effects are most often registered during strong earthquakes and especially in case of critical frequency of ground motion, which is not known in advance and cannot be reliably predicted. In some critical circumstances, current seismic isolation systems of bridge structures can be exposed to serious damage that may pose threat to general stability of the structure. Various disadvantages of the existing technological solutions may individually or cumulatively be the reason for large problems and unacceptable disturbance to the stability of bridges under the effect of earthquakes, which rank among the most critical and unpredictable natural phenomena as to their intensity and frequency. Typical abrupt

damage to seismically isolated structure was recorded during the strong earthquake in Duzce, Turkey in 1999. Extensive damage to the large Bolu viaduct was mainly due to the recorded ruptured fault that crossed the viaduct producing earthquake that was significantly stronger than the design earthquake. However, the isolated structure resisted total collapse and, following successful repair works, it was restored to operation. Considering the fact that seismically isolated structures can be exposed to high risk in some specific seismic circumstances, the present research was originally devoted to development of an improved system for seismic upgrading of isolated bridges.

2.2. Integrated experimental research program

An extensive experimental and analytical research was realized at the Institute of Earthquake Engineering and Engineering Seismology (IZIIS) in Skopje within framework of the three year NATO Science For Peace and Security Project: *Seismic Upgrading of Bridges in South-East Europe by Innovative Technologies (SFP: 983828),* integrally guided by the third author (Ristic, D.) in period 2010-2014. The project was focused on fundamental research and development of innovative technologies for seismic isolation and seismic protection of bridges. The experimental tests and study that have been directed toward development of the presently introduced USI-SF system actually represent one specific study segment of the extensive research carried out in the frame of the NATO Science for Peace and Security Project.

2.3. Concept of advanced USI-SF system for seismic protection of bridges

The upgraded seismically isolated (USI) system with the space flange (SF) energy dissipation (ED) devices is an advanced technical concept providing harmonized and improved modification of structural seismic response. The USI-SF system was created as an advanced alternative method for qualitative improvement of seismic protection of bridge structures and it constitutes an integrated adaptive system based on the introduced concept of global optimization of seismic energy balance. The USI-SF system was created through obligatory incorporation of the following three harmonized complementary systems:

Incorporation of seismic isolation (SI) system
The system applied for seismic isolation of bridge superstructure should contain adequately selected seismic isolators that will provide quite low stiffness in horizontal direction and that will be capable of sustaining safely the total weight of the entire superstructure resting upon the SI devices. In that way, an appropriately designed seismic isolator can be installed at each supporting point of bridge superstructure whereas the total isolated weight is directly transferred to the supporting middle piers and/or to the rigid supporting abutments of the bridge. In this case, there are ample possibilities for selecting proper system for seismic isolation of bridge superstructure, including application of any newly developed advanced technical solution for seismic isolation.

Incorporation of seismic energy dissipation (ED) system
Seismic isolators are characterized by insufficient damping for seismic energy dissipation, and so additional seismic energy dissipaters have been introduced. For this reason, the ED devices should exhibit an optimum stiffness, optimum bearing capacity and high ductility as related to seismic performance of seismic isolators. First, very large stiffness of ED devices leads to undesired impact and impulsive transfer of inertial forces. To avoid this problem, it is advisable to reduce the initial stiffness of ED devices to an optimum level. Second, if the bearing capacity of ED devices is very high, they will possibly transfer large or critical forces to the piers. To avoid the related problem, the bearing capacity of energy dissipaters should be reduced to a design limit. Third, the ductility capacity of ED devices should be sufficiently large. In case of large inertial forces, relative displacements can become very large, of the order of 25-30 cm or larger. Therefore, the ED devices should be able to sustain large deformations without damage. Generally, it is necessary to introduce ED devices exhibiting greater capacity of seismic energy dissipation through nonlinear deformation and creation of pronounced hysteresis curves. Very significant advances of the three above specified properties were achieved in the framework of this study by formulation of the proposed advanced SF-ED devices.

Incorporation of displacement limiting (DL) system
A limited number of pronounced strong impulses are likely to occur in the course of strong earthquake vibrations. In that case, very pronounced displacement amplitudes may occur, and sometimes they are not successfully controlled in a reliable engineering manner. Strong impact and negative effects should be reduced or altogether avoided by introducing specific displacement limiting devices (DLD).

2.4. Research methodology

The first part of the experimental research included nonlinear cyclic quasi-static tests of prototype models of the advanced components and devices, which were installed for this testing directly on their real locations within the constructed large-scale ISUBRIDGE prototype model. The second part of the experimental research included seismic testing of the USI-SF bridge model under the simulated strong earthquake action on a seismic shaking table. By applying special design considerations, the same physical model was made compatible for successful quasi-static testing of individual devices, and seismic testing of the USI-SF bridge model on the seismic shaking table.

3. Testing prototype models of novel DSRSB isolation devices

3.1. Experimental validation program for DSRSB devices

It was originally planned to conduct experimental validation of seismic performance of the advanced USI-SF system for seismic protection of bridges through an extensive shaking-table testing of an originally built large scale bridge prototype model, under simulated effects of recorded real-life strong earthquakes. However, the originally planned type of seismic isolation bearings was not available for purchase. To overcome this problem, it was necessary to realise an extensive preparatory research process involving original design of scaled prototype models of specific seismic isolation bearings, their first production and their original experimental testing under simulated reverse cyclic load. The research conducted in this study phase involved the use of an improved seismic isolation system for bridge modelling, by introducing double spherical rolling seismic bearing (DSRSB) devices.

3.2. Design of DSRSB prototype models

The seismic isolation system applied in the construction of the USI-SF bridge model, experimentally tested on a seismic shaking table, was assembled using the constructed advanced prototype models of double spherical rolling seismic bearing (DSRSB) devices with two spherical surfaces with a large radius, Figure 1, Figure 2, and Figure 3. Special design requirements were set out in the design of the prototype models of DSRSB devices:

- provide sufficient bearing capacity for vertical loads for planned experiments
- provide sufficient displacement capacity for planned experimental tests
- provide an adequate radius of curvature of spherical surfaces needed for achieving test target period of vibrations
- provide sliding surfaces with minimum friction
- design and produce the central rolling part exhibiting a minimum reactive friction force.

All dimensions of the DSRSB prototype device were defined in accordance with all requirements set to that effect.

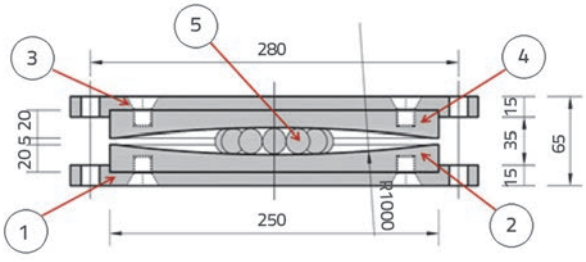

Figure 1. Prototype of DSRSB device: cross-section with geometrical properties

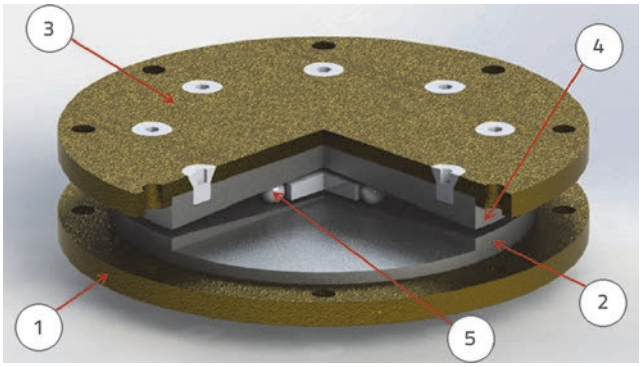

Figure 2. Prototype of DSRSB device: view of device with characteristic cross-section

The upper (4) and the lower (2) spherical plates, Figure 1, were made of an appropriate type of hard stainless (non-corrosive) metal exhibiting durability and polishing to a mirror shine, which results in minimization of the friction coefficient. The central rolling part (5) was appropriately designed in form of a ring with 12 rolling balls 18 mm in diameter, symmetrically positioned along a circle, with their centres 74 mm away from the centre of the circle. The radius of spherical surfaces of the upper and the lower plates amounted to R = 1000.00 mm. The central rolling part was constructed in form of a cylindrical ring 80.0 mm in diameter. The distance between the two spherical plates amounted to h = 5.0 mm at the edge. The upper (4) and the lower (2) spherical plates were constructed with a diameter of D = 250.0 mm, while the thickness of the outer side amounted to d_1 = 20.0 mm. Both spherical plates were fixed to the upper (3) and lower (1) end metal plates 310.0 mm in diameter and 15.0 mm in thickness. Eight openings 14 mm in diameter were made along the circumference of both end plates, Figure 3. These openings served for installation of seismic bearings. A series of eight prototype models of DSRSB devices were produced to enable assembly of optional bridge test models, including a model with three spans and eight support points, (Figure 1, Figure 2, and Figure 3). The number of DSRSB devices depends on the number of spans of the bridge test model. Four of them were needed for the tested one span bridge, using two devices at each end support position.

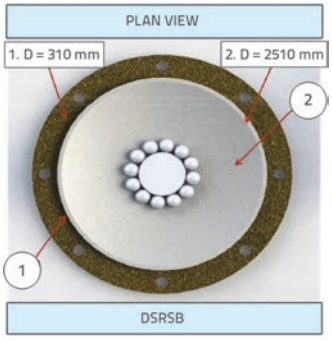

Figure 3. Prototype of DSRSB devices: plan view with main geometrical properties

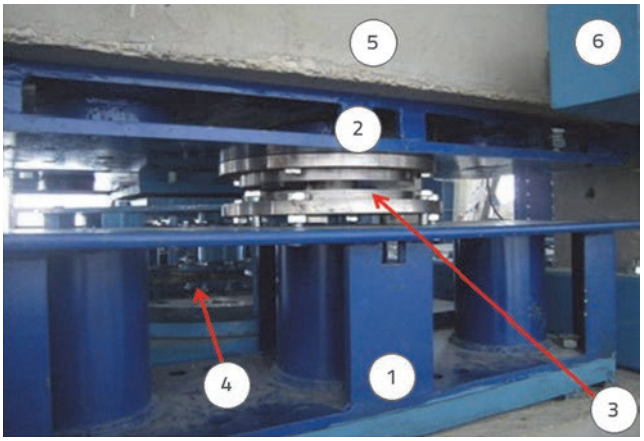

Figure 4. Prototype of DSRSB device installed in a large-scale USI-SF bridge test model

The first production of DSRSB prototype models was completed based on original design using very specific industrial processes. Seismic bearings exhibit a high bearing capacity for vertical load amounting to max N = 200 kN, each. However, their fundamental period of vibrations does not depend on the amount of vertical load, and so they can be used for many seismic tests (applying different load levels) in laboratory conditions. Production process for the first eight prototype models included several successive activities:

- procurement of steel material
- manufacturing of standard steel elements
- procurement of a hard stainless metal
- accurate manufacturing of spherical stainless metal plates
- polishing of sliding spherical surfaces to mirror shine
- connection of ready-made parts,
- installation of novel prototypes and testing.

3.3. Testing of hysteretic behaviour of DSRSB prototypes

The most suitable experimental set-up was applied for the testing of DSRSB devices (Figure 4) profiting from the fact that the substructure and superstructure (5) of the bridge test model were already built, following the previously defined integral test programme. Then the four prototype DSRSB devices were directly incorporated at their real positions, two at the left-side abutment and two at the other abutment. In this way, the RC slab (5) of the superstructure of the model rested through steel connecting part (2) on four seismic bearings (3) with its weight of Q = 85.0 kN. Accordingly, its total weight exerted the actual vertical force of F_z = 21.25 kN upon each individual bearing.

The planned quasi-static tests were successfully accomplished using a hydraulic actuator (6) shown in Figure 5, originally designed with large capacity of displacement stroke, applicable for inducing any predefined displacement history with large displacement amplitudes, up to maxD = ± 300 mm. In addition, the implemented actuator exhibits an optimum capacity for application of reverse forces, up to maxF = ± 300 kN.

The programmed horizontal cyclic loads were very successfully applied directly upon the superstructure RC slab by an actuator (6) fixed to the right support (2) of the bridge model substructure, by means of a suitable metal structure (5) constructed for that purpose, Figure 5. Such an experimental assembly had many advantages since it enabled application of identical vertical loads, or real loads used in planned seismic tests, and finally it enabled successful simulation of the programmed history of cyclic displacements with an increasing amplitude up to the necessary limit of maxD = 45.0 mm. The conducted experimental quasi-static testing of hysteretic behaviour of prototype devices, using already constructed segments of large-scale bridge model anticipated for seismic testing, represented the most consistent way for simulating real nonlinear characteristics of tested prototypes, Figure 5.

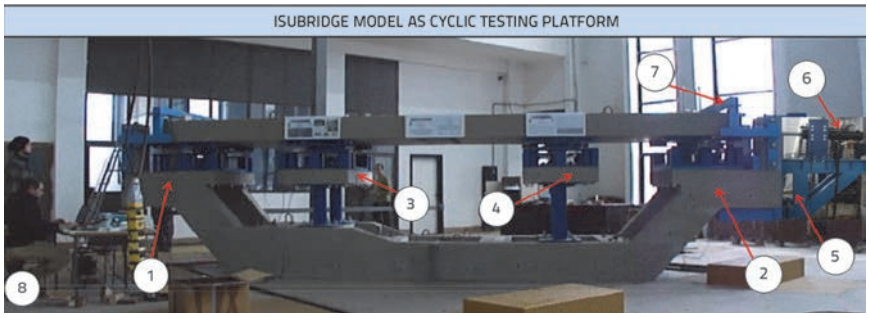

Figure 5. USI-SF bridge model used for testing of DSRSB and SF-ED devices under simulated reversed cyclic loads: (1) left end support; (2) right end support; (3) support above shorter middle piers; (4) support above longer middle piers; (5) steel structure supporting actuator; (6) actuator for application of cyclic loads; (7) steel structure supporting DL devices; (8) computer control system

Real representative hysteretic characteristics of a single device were defined analytically using the recorded experimental results for the tested set of four DSRSB devices, and by dividing the recorded force by 4. A representative hysteretic response of a single DSRSB device prototype is shown in Figure 6. The recorded response curve had to be shifted because the presented test was started with displacement set to zero, following a previously completed test from which some force level was still present. The results show that the shape of the hysteretic response forms an inclined rectangle and can be very successfully modelled by a bilinear model. In addition, the capacity for horizontal deformation of this seismic bearing, amounting to ≥ 45.0 mm, is also sufficient. From the defined hysteretic relationship, it can be concluded that the seismic isolation system composed of DSRSB devices exhibits excellent characteristics manifested by:

- very small reaction force in all horizontal directions
- very small rolling friction force
- very stable hysteretic curve for the entire range of large displacements.

The total weight of the bridge model superstructure was Q = 85.0 kN. The hysteretic response record of one DSRSB device shows very low maximum resistance amounting to: maxF = ±0.90 kN or, in percentage, it amounts to: pf = maxFx100/(0.25xQ) = 4.2 %. The recorded experimental data reveal that the tested DSRSB isolation device has a very stable hysteretic behaviour in all directions and exhibits extraordinary characteristics for seismic isolation of structures through its capability of avoiding possible resonance state under the strongest seismic excitations. The SF-ED devices were not present during hysteretic behaviour testing of the DSRSB isolation system. In this way, only the real hysteretic behaviour of the integral DSRSB seismic isolation system was recorded.

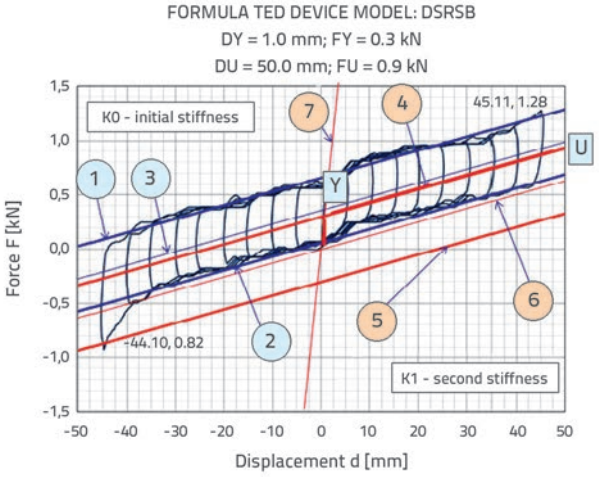

Figure 6. Nonlinear hysteretic response of one DSRSB prototype model: (1) recorded upper envelope curve (EC); (2) recorded lower EC; (3) recorded symmetrical line; (4) shifted upper EC; (5) shifted lower EC; (6) shifted symmetrical line; (7) recorded initial stiffness

3.4. Conclusions from tested prototypes of DSRSB devices

The following conclusions can be made based on the detailed study of seismic behaviour of novel double spherical rolling seismic bearings with spherical surfaces of identical large radius:

- These DSRSB devices require accurate proportioning so that they can sustain expected vertical loads
- Fundamental period of these bearings depends on the radius of spherical surfaces
- Rolling seismic bearings have a large capacity for horizontal displacement
- Hysteretic response of DSRSB devices was very stable with a shape of an inclined rectangle
- Bilinear model can be applied very successfully for analytical modelling of DSRSB devices
- DSRSB isolation devices subjected to testing have a great potential for use in engineering practice.

4. Testing prototype models of advanced SF-energy dissipation devices

4.1. Experimental validation program of SF-ED devices

The seismic energy dissipation system installed in the tested USI-SF bridge model was composed of the advanced steel space flange (SF) energy dissipation (ED) devices. SF-ED dissipation devices of the proposed type have not been studied before and were not available on the market. A part of research devoted to development of two basic shapes of system-1 SF-ED devices, i.e. SF-ED-8C-L1R and SF-ED-4C-L1R, is included in the paper. This research provided some important outcomes:

- technology for design, production and testing of SF-ED devices was mastered
- real characteristics of hysteretic behaviour used in formulation of analytical models were obtained
- adequacy for installation in the large-scale bridge model for dynamic testing on a seismic shaking table was confirmed
- conditions were created for validation of the USI-SF system on the experimental shaking table.

4.2. Design of SF-ED prototype models

Two basic shapes of the SF-ED device, i.e. SF-ED-8C-L1R-Ti and SF-ED-4C-L1R-Ti, were created with an important precondition of achieving spatial and harmonized reaction of the device in all directions. The labels used determine more closely the actual device: SF - space flange; ED - energy dissipation; 8C or 4C-number of components; L1R - actual dimension L = 1R, and T1 or T2 actual cross-sectional dimensions of the installed components. The trajectory of the imposed relative motion of bridge superstructure with respect to bridge substructure during an earthquake event is unknown or highly unpredictable. Structural response under earthquake motion belongs to the category of random vibrations. A spatial spherical device structure was adopted to enable spatial reaction of the device. This structure consists of eight or four symmetric SF-ED steel components fixed at upper support plate (USP) and lower support plate (LSP) that are used for fixing the device in the USI-SF bridge prototype model, in the gap between the RC superstructure and substructure (Figure 7, Figure 8, Figure 9, and Figure 10). Basically, eight steel components are placed radially at 45^0 in the defined xy coordinate system.

Eight SF-ED components were selected for the complete SF-ED device so as to achieve nearly equal harmonized reaction in all arbitrary earthquake directions, Figure 7.

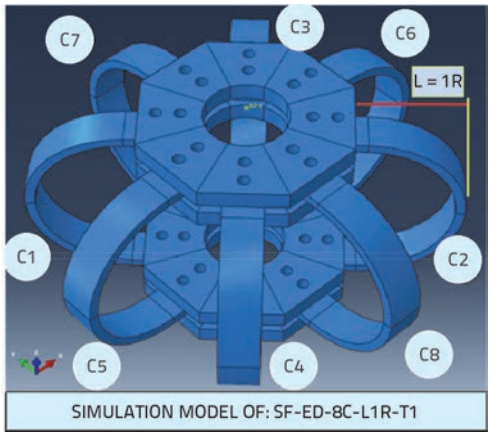

Figure 7. Prototype model of basic SF-ED-8C-L1R-T1 device

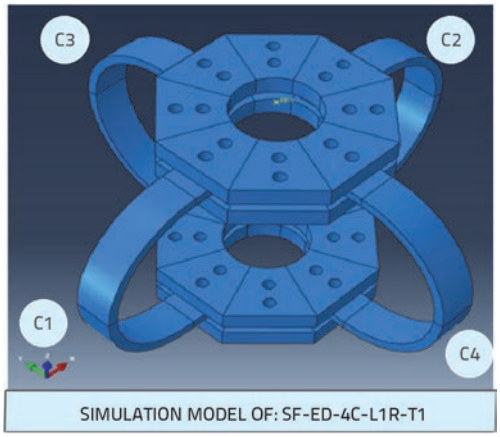

Figure 8. Prototype model of basic SF-ED-4C-L1R-T1 device

The radial steel prototype components (5), Figure 9, are constructed in form of space flanges (SF) with a rectangular cross-section. The cross-section of space flanges Ti can be variable. Mechanical characteristics of the applied metal can also be variable. With variation of cross-section proportions of the flanges and mechanical characteristics of the steel, conditions are created for the elaboration and production of SF-ED devices of desirable initial stiffness, ultimate strength, ductility capacity and displacement capacity. The fixing of the upper (3) and the lower (1) contact surfaces of ED devices, Figure 9, can be realized using different structural solutions defining different boundary conditions for the joint connections (2) and (4). Based on possible variations of boundary conditions, cross-sections of spherical flanges, and mechanical properties of the selected steel types, wide opportunities have been opened for industrial production of a large range of ED devices of SF-class. The space flanges (5) have a semi-circular form, while their external radius is R = 105 mm (external diameter is D = 210 mm). To provide conditions for fixing space flanges (ED components) at the upper and the bottom ends, Figure 9, horizontal parts of the flange (5) were designed in form of extensions with a length of Lf = 70 mm each. Two openings 12 mm in diameter were made in each of these extensions for the purpose of efficient fixation of both ends of space flanges between two octagonal steel plates located on the upper side of the fixation (4) and analogue two identical steel plates located on the lower side of support (2). Four octagonal steel plates were constructed as identical with side dimension a = 87 mm and thickness d = 20 mm. The assembled respective type of SF-ED devices is fully fixed to the bridge model superstructure and substructure using the upper and lower end connecting systems (Figure 9 and Figure 10). Space flanges in SF-ED devices have two different cross-sections, b/d = 40/10 mm and b/d = 40/8 mm, denoted with labels T1 and T2, respectively.

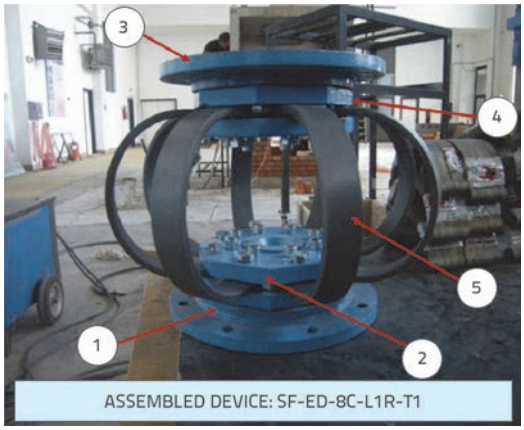

Figure 9. Assembled basic device SF-ED-8C-L1R-T1: (1) lower base plate; (2) lower support plates; (3) upper base plate; (4) upper support plates; (5) SF-ED component

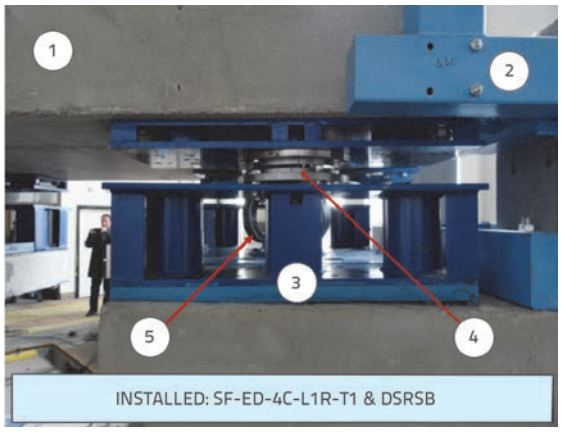

Figure 10. Detail of devices ready for testing: (1) superstructure; (2) steel support of DL-device; (3) steel support of DSRSB device; (4) DSRSB device; (5) SF-ED-4C-L1R-T1 device

The first production of the basic prototype models of SF-ED devices was realized based on original designs. All metal parts, components, connection systems, and optional model devices were produced and used for realization of original quasi-static tests and dynamic shaking table experimental research phases. The process of the first production of the prototype models of SF-ED devices (Figure 9) involved important activities, including:

- procurement of ductile steel material
- manufacturing of all steel elements and devices
- construction of specific connecting steel parts used in the USI-SF bridge model
- manufacturing of supporting steel structure used for installation of mobile actuator for cyclic testing, Figure 5
- production of specific connecting metal parts.

4.3. Testing hysteretic behaviour of SF-ED prototypes

With the considered innovative space structure characteristics of SF-ED devices, the activation of all eight or, alternatively, all four installed space flanges (components), was enabled in case of induced displacement in any direction, depending on the direction of the resultant seismic force. Considering the actual orientation, the contribution of various SF-ED components to the imposed cumulative restoring force of SF-ED device is different, and depends on actual radial direction of ED flange (component) with regard to the direction of resultant deformation. Generally, if the direction of the deformation coincides with the orientation angle of a single component, then the input deformation generates change of geometrical shape of that SF-ED component. In the first phase, the component is gradually transformed from the initial semi-circular form into asymmetric semi-elliptical form. The asymmetry of the semi-elliptical form is the result of relative motion of two parallel support plates. In the course of larger deformations to the SF-ED component, the component is exposed not only to bending but also to tension at one end, while compression dominates at the other end. The induced complex distribution of stresses, Figure 16, results in respective change of the device geometry. Consequently, complex nonlinear response of the SF-ED component is observed, especially in case of considerable increase in relative deformations. If the direction of relative deformation does not coincide with the direction of a particular SF-ED component, for example, if the angle is $\alpha = \pm 45^{o}$ or $\alpha = \pm 90^{o}$ or $\alpha = \pm 135^{o}$, then the component is additionally exposed to torsion and so the resultant stress distribution in different cross-sections becomes even more complex. However, the experimental tests provided the opportunity of determining the real nonlinear behaviour of both, individual ED components installed in different geometrical positions as well as of assembled complete SF-ED devices. In practical applications, the proposed SF-ED device can be assembled as a unit with eight ED components (C1 to C8), Figure 7, or as a unit with symmetric assemblage of four ED components (C1 to C4), Figure 8. In both cases, the upper and the lower metal plates to which the upper and the lower ends of the SF-ED device are fixed move in parallel and may achieve quite large relative deformations adequate to the capacity of deformation of the applied seismic isolators in the USI-SF bridge system. Therefore, nonlinear behaviour of various SF-ED components of the SF-ED devices represents a complex stress-strain state produced due to deep material nonlinearity and large effect of geometrical nonlinearity manifested as a result of large change in initial geometry of each individual SF-ED component. Considering the achieved creation of many different and special applicability options, the presently designed and constructed large-scale USI-SF bridge prototype model served very successfully as specific self-adaptable experimental testing platform (SA-ETP), Figure 5. The created SA-ET platform provided condition for realizing many different quasi-static tests (more than 100), including hysteretic behaviour tests of different configurations of SF-ED components and SF-ED devices. The planned quasi-static tests were successfully realised using a hydraulic actuator (6), as shown in Figure 5. All experimental tests were performed automatically using the predefined history of cyclic displacements with increasing displacement amplitudes up to deep nonlinearity. In that way, advanced conditions were created for generation of original hysteretic diagrams for all tested configurations, after excluding known participation of the present rolling isolation system composed of four previously tested DSRSB devices. In this original way, the advanced USI-SF bridge system was composed and considered in the scope of present experimental and analytical study. Actually, the superstructure of the bridge model in form of a heavy RC slab was installed above the four DSRSB devices representing a seismic isolation system. Some representative results obtained by testing hysteretic behaviour of different configurations of SF-ED components are presented in Figures 11 and 12. The typical nonlinear hysteretic behaviour of a pair of SF-ED components, installed under an angle of α ±45°, is presented in Figure 11. Analogously, Figure 12 shows typical nonlinear hysteretic behaviour of the same pair of SF-ED components, but for their characteristic position defined by an angle of α ±90°. The experimentally obtained hysteretic diagrams show that the SF-ED components possess favourable characteristics as follows: (1) Hysteretic relationships of every symmetrically assembled pair of SF-ED components are very stable; (2) Due to considerable change of initial geometry, the SF-ED components showed a pronouncedly stable second stiffness K2 in the second phase.

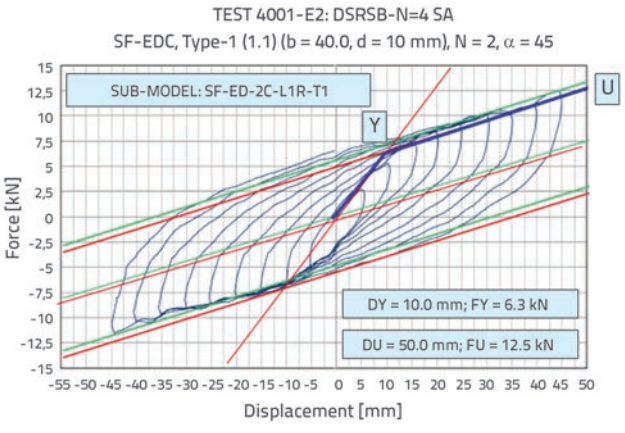

Figure 11. Hysteretic response of two SF-ED components type-T1 (α = ±45 °)

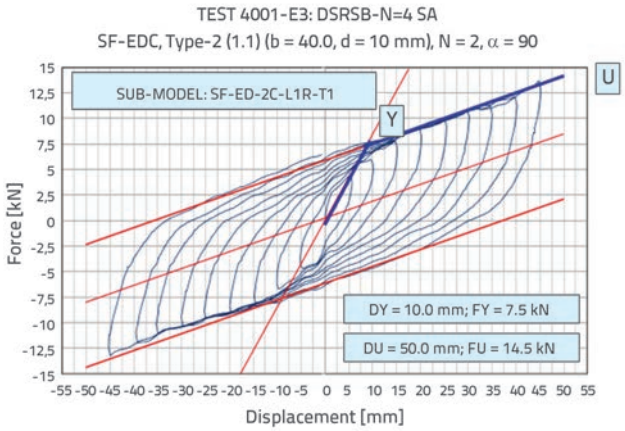

Figure 12. Hysteretic response of two SF-ED components type-T1 (α = ±90 °)

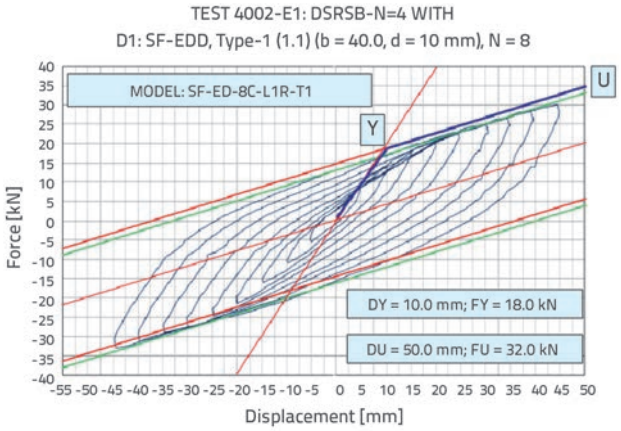

Figure 13. Hysteretic response of original SF-ED-8C-L1R-T1 device with eight (N = 8) components

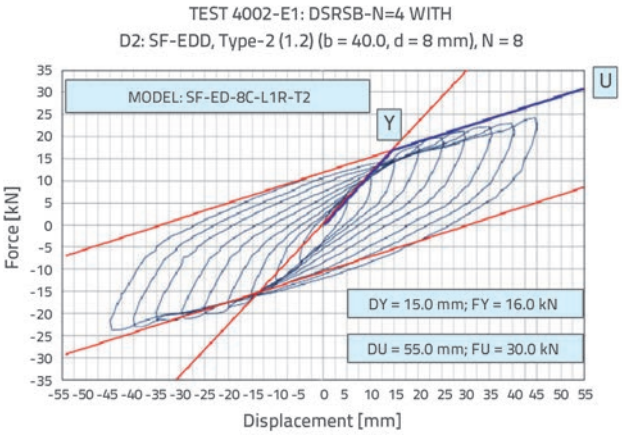

Figure 14. Hysteretic response of original SF-ED-8C-L1R-T2 device with eight (N = 8) components

Their initial stiffness K1 is higher, but the yielding point is reached under relatively small deformations. After that, a pronounced nonlinear behaviour, characterized by considerable enlargement of the areas of hysteretic cycles, is initiated.

Such a characteristic reveals the possibility of large absorption and dissipation of seismic energy by SF components within the entire range of large cyclic deformations; (3) Upon reversing from each achieved maximum deformation in any direction, the small reverse elastic deformations are again manifested and, immediately after that, the element is once again activated in nonlinear range, creating a hysteretic response; (4) Hysteretic relationships are very stable and show large capacity for seismic energy dissipation. In addition to their original basic geometrical characteristics, it is possible to change their shape in order to obtain a new technical solution; (5) In accordance with the adopted identical geometrical characteristics of the tested pairs of components, similar values of maximum resistance forces were obtained in both tests as follows: (1) for test-1 (α ±45°), the maximum resistance force amounts to Fmax = ± 12.5 kN and (2) for test-2 (α ±90°), the maximum resistance force is somewhat higher and reaches the value of Fmax = ± 14.5 kN. With these specific investigations, it was confirmed that the design engineer has an open option to design typified elements for seismic energy dissipation with optimally defined nonlinear characteristics. Consequently, the final quasi-static testing included experimental testing of full SF-ED devices. Figure 13 shows a hysteretic diagram of a tested SF-ED-8C-L1R-T1 device composed of eight SF-ED components of type T1. The results from this test show that the maximum resistance force reaches the value of Fmax = ± 32.0 kN, while the shape and stability of hysteretic curve are completely preserved and exhibit very good characteristics. Figure 14 shows a hysteretic curve of the tested SF-ED-8C-L1R-T2 device composed of eight energy dissipation components of type T2. The recorded maximum force is somewhat smaller (Fmax = ± 30.0 kN), but the characteristics of the hysteretic response are also highly favourable.

4.4. Conclusions after testing SF-ED prototypes

Based on quasi-static test results for prototype models of SF-ED components and SF-ED devices, the following can be concluded: (1) The proposed original concept of SF-ED devices with activation of nonlinear response of space flanges represents an attractive compact solution with favourable behaviour and wide application possibilities; (2) Application of devices in real bridges can be successfully defined during the design process by adopting a correct set of geometrical and material properties; (3) Braking and wind forces may be fully controlled by adding some common elements; (4) The efficient and stable activation of SF-ED devices in all directions is an advanced feature since it protects the system integrity and does not allow an earthquake to detect "weak points" of the isolated structure; (5) The seismic isolation system with double spherical rolling seismic bearings provided equal response in all directions and was characterized by a very stable behaviour even under largest amplitudes of induced displacement.

5. Numerical simulation models of advanced SF-ED devices

Analytical simulation of cyclic nonlinear behaviour of the proposed basic SF-ED-8C-L1R-T1 prototype device constituted a highly complex modelling task due to complex 3D geometrical shape of the device and specific boundary and/or installation conditions. An advanced theoretical background is essential to achieve realistic analytical simulation of nonlinear hysteretic response of the device, and analysis of nonlinear seismic response of the tested bridge model (in phase-2). Advanced achievements are needed in the field of general matrix analysis of structures [28], nonlinear finite element method [29, 30], dynamics of structures with numerical methods for nonlinear step-by-step analysis of structures, [31, 32], and an advanced scientific background in the field of material science and bridge engineering is also required, [33, 34]. Advanced special purpose analysis programs have been studied and used [35-37] to practically realize the planned very complex nonlinear 3D cyclic response analysis of the novel SF-ED devices, and nonlinear 3D seismic response analysis of the advanced USI-SF bridge model. A nonlinear 3D analytical model formulated using ABAQUS computer software is used in this initial phase for numerical simulation of hysteretic response of the advanced SF-ED devices [36]. If the material is considered as linearly elastic, if boundary conditions remain unchanged, and if only one set of external forces is slowly applied to the structure, the analysis corresponds to a single linear static solution. In such a case, only one set of equilibrium equations needs to be solved, if boundary conditions are imposed:

$$[K]\{U\} = \{R\}$$

If the problem is not linear and if the stiffness matrix is not constant, it is necessary to use a nonlinear analysis involving a number of iterations to obtain equilibrium solution of specified accuracy, for each loading case.However, the analysis of hysteretic response of complete SF-ED-8C-L1R-T1 device required solution of a complex nonlinear problem considering the specific procedure of multiple loading case. The prescribed loading was numerically simulated with 30000 loading steps and a number of equilibrium iterations were made in every step to achieve the prescribed solution accuracy. The conducted study is highly useful as it provides an important general tool for solving specific problems, including:

- validation of capability of the implemented refined 3D nonlinear modelling concept for solving specific research and design tasks
- experimental validation of the proposed model for simulation of complex hysteretic response of SF-ED-8C-L1R-T1 device under general cyclic loading up to deep nonlinearity.

The integral research activities in this domain were successfully realized in three consecutive phases:

- formulation of nonlinear refined 3D analytical model
- analysis of nonlinear hysteretic response of the device under simulated cyclic deformations
- comparative presentation of original theoretical and experimental results.

a) Formulation of the refined nonlinear analytical model of the SF-ED-8C-L1R-T1 prototype device. Figure 15 shows an example of the formulated refined three-dimensional nonlinear finite element model (R3DNL-FE model) of the complete device of type SF-ED-8C-L1R-T1, used for nonlinear analysis with the ABAQUS computer program [36]. Fixed boundary conditions are ideally simulated for the bottom support plate. A permanent horizontal position was prescribed for the upper plate during the simulated cyclic deformation in x-direction representing real input for numerical simulation of nonlinear cyclic behaviour of the modelled device.

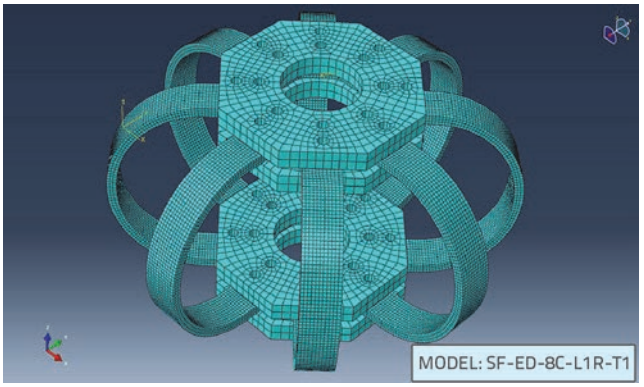

Figure 15. Refined 3D nonlinear FE model implemented for analytical simulation of complex hysteretic response of present SF-ED-8C-L1R-T1 device

b) Analysis of nonlinear hysteretic response of the SF-ED-8C-L1R-T1 prototype device. An available option for incremental nonlinear static analysis was implemented to perform this type of specific quasi-static time dependent analysis. It enables simulation of incremental deformation in the specified direction. For that purpose, a known predefined history of cyclic displacements, similar to that used during realization of the corresponding experimental test, was numerically specified and analytically applied. Appropriate history of deformation increments in incremental analysis with adopted iterative nonlinear solution procedure, considering additional step-based iteration process for the achievement of specified accuracy, was analytically considered based on the known predefined history of cyclic deformations. Complete nonlinear-analysis results were obtained in the refined numerical form for all relevant physical values (stresses, strains, forces, deformations, etc.) using a detailed nonlinear analytical micro-model. Typical stress distribution in all SF-ED components during the simulated actual mechanical response under

induced incremental relative displacement between bottom and top supports of the complete SF-ED device of the type SF-ED-8C-L1R-T1 is presented in Figure 16.

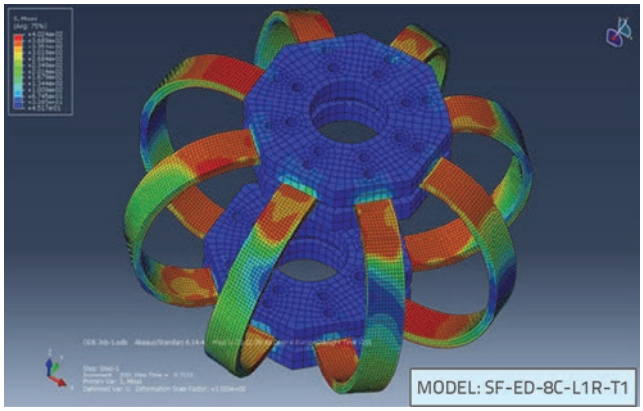

Figure 16. Stress distribution in SF-ED components during hysteretic response of advanced SF-ED-8C-L1R-T1 device under induced relative cyclic displacements up to deep nonlinearity

c) Importance of experimental and theoretical results. A very stable hysteretic diagram was obtained from the experimental test of the same device up to deep nonlinearity, as can be seen in Figure 17. In case of testing, the actual level of fixation of all ED device components, between lower and upper steel support plates, was realized by applying a predefined torsion moment Mt = 0.4kNm to all bolts, thus achieving semi-fixed support conditions. Considering relevant experimental results, the resulting bi-linear representative envelope was defined as shown in the same figure. A complete analytically obtained hysteretic response of the SF-ED-8C-L1R-T1 device under reversed cyclic loads, computed with formulated refined 3D nonlinear model, is presented in Figure 17.

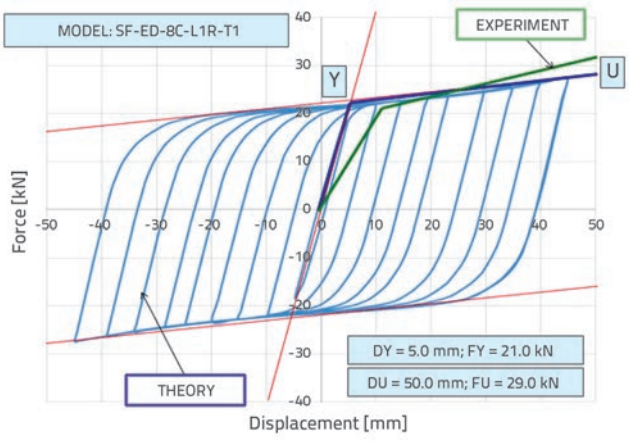

Figure 17. Hysteretic response under reversed cyclic loads of SF-ED-8C-L1R-T1 device computed with formulated refined 3D nonlinear FE model simulating perfectly fixed SF-ED connections

However, in this analysis, the perfectly fixed bottom and top support conditions were simulated analytically. As shown in Figure 17, the hysteretic response of the device is very stable, with ideal symmetry showing very high computation accuracy. However, some difference can be seen during comparison of the simple experimental bi-linear envelope and the analytically defined bi-linear envelope. The analytical hysteretic curve is wider in comparison to the experimental one, but a good simulation of complex actual response characteristics was achieved. This difference basically results from analytically simulated ideally fixed support connections of SF-ED components, instead of actual semi-fixed conditions, not considered in the present study. However, it was confirmed that the application of the refined 3D nonlinear analytical model is the most powerful, generally applicable and highly advanced modelling option, capable to realistically simulate complex nonlinear hysteretic response of SF-ED devices. The implemented modelling approach represents the advanced modelling option, providing conditions for its further upgrade to cope with analytical simulation of complex construction and structural details. Finally, the application of the experimentally verified concept for refined nonlinear analysis of geometrically complex components and devices up to deep nonlinearity opens an extraordinary opportunity for introducing the advanced systems for qualitatively improved seismic protection of bridge structures by optimum modification of seismic response of the system.

6. Shaking table tests of USI-SF bridge model under strong earthquakes

6.1. Concept of shaking table USI-SF bridge prototype model

The strategy for planning and building physical models involves study of several important aspects concerning simulation of main geometrical, physical and behaviour characteristics of selected prototypes, as related to actual conditions for dynamic testing on the IZIIS seismic shaking table. Therefore, the dimensions of the prototype bridge constituent elements and their contribution to global performance of the bridge prototype, the characteristics of main structural components, type of the implemented seismic isolation system, characteristics of the installed original SF-ED devices and their interconnections, and the building processes used in the prototype, were taken into account in the design and construction of the presently tested physical models. The total length of the considered three span prototype bridge is L = 15.75+27.00+15.75 = 58.50 m. Its continuous RC bridge superstructure was supported on piers through hinge type supports, but movable bearings were used at both bridge end supports. The height of the shorter and longer piers was h_1 = 9.50 m and h_2 = 11.70 m, respectively. In the bridge prototype model design, the seismic gap was considered with

Table 1. Design parameters of the 1/9 scale model of USI-SF prototype bridge implemented in shaking table tests as combined option of true replica-artificial mass simulation model

No.	Scaling parameters	Required scaling factors	Required scaling factors for *lr* = 1/9	Adopted scaling factors for *lr* = 1/9
1	Length (*lr*)	*lr*	1/9	1/9
2	Time (*tr*)	$(lr)^{1/2}$	1/3	1/3
3	Gravitational acceleration (*gr*)	1	1	1
4	Acceleration (*ar*)	1	1	1
5	Velocity (*vr*)	$(lr)^{1/2}$	1/3	1/3
6	Frequency (*fr*)	$(lr)^{-1/2}$	3	3
7	Displacement (δr)	*lr*	1/9	1/9
8	Weight (*Wr*)	$(lr)^{3}$	1/729	1/729
9	Force (*Fr*)	$(lr)^{2}$	1/81	1/81
10	Moment (*Mr*)	$(lr)^{3}$	1/729	1/729
11	Period (*Tr*)	$(lr)^{1/2}$	1/3	1/3

the intentionally extended height of h_g = 40.0 cm in order to create conditions for installation of devices with dimensions suitable for the present specific research purposes. In reality, their geometry as well as behaviour characteristics can be adjusted accordingly. Considering all related factors, primarily the seismic shaking table size (5.0 x 5.0 m) and payload capacity, the basic ISUBRIDGE model had to be geometrically reduced from the original prototype. For these reasons, a geometrical scale factor of 1:9 was adopted, which verified the referred constraints in this case, but with the adopted specific model design concept. As a consequence of this scale reduction, all phenomena involved in the dynamic tests that were being set were scaled according to the similitude law [23]. An adequate model (combined true replica-artificial mass simulation model) was adopted taking into account main relevant factors. For the stiff RC superstructure simulation, the stiff slab with added mass (through increase in cross section dimensions) was adopted using the same material as that of the prototype structure. Steel material was used for simulation of middle piers. The seismic isolation and energy dissipation devices were designed and produced on a reduced scale. The similitude law implies the adopted relations for various parameters, all given in terms of the geometrical scale factor (*lr*), Table 1. Concrete material type C25/30 was used in construction of RC segments of bridge model, while steel material type S355 was selected and applied for the construction of steel SF-ED devices. Considering the above design parameters, the experimental model of the bridge was primarily conceptualized in such a way to create realistic conditions for successful fulfilment of the already stated main research objectives, [24-27]. It primarily includes experimental validation of actual seismic performance of the USI-SF system under effects of very strong earthquake excitations. A large-scale physical model of the typical prototype bridge with three spans was used to meet the stated objectives. During the design and construction of the bridge model, few important initial goals were established to ensure safe simulation of high level of inertial forces producing sufficiently strong response of the system.

The most important preconditions were selected as follows:

- Three spans were adopted for the prototype bridge in order to enable existence of rigid abutments and flexible middle piers, which is very common and characteristic option of real bridge structures constructed in engineering practice
- Central piers of the prototype bridge should exhibit appropriate flexibility (much greater than the one exhibited by rigid abutments) in order to include the realistic phenomenon of rigid abutments and flexible central piers at some different experimental tests to be conducted in the future
- Different central pier heights were assumed so as to provide for different stiffness of such central piers. This enabled that the same model of the prototype bridge can be applied for experimental testing of bridge having rigid abutments and central piers of different stiffness
- The superstructure of the model of the prototype bridge was designed as a rigid RC deck with an adequately defined total weight to enable simulation of realistic large inertial forces without applying additional load, Figure 18. This enabled activation of the installed DSRSB devices and SF-ED devices
- Direction of earthquake ground motion is not known in advance and generally should not directly coincide with the main directions of the bridge, either longitudinally or transversely. For these reasons, the longitudinal axis of the bridge was positioned diagonally as related to the square shape of the shaking table. In that way, generation of seismic forces was enabled in both, longitudinal–x and transverse-y directions, although the IZIIS' seismic shaking table applies the seismic input in vertical and one horizontal direction

- Bridge superstructure completely rests on the DSRSB seismic isolation system. In that way, the total weight of the superstructure is transferred to the supporting points, represented by seismic isolators
- The seismic SF-ED devices are conceptualized in such way that they will not participate in sustaining any weight. The only role of SF-ED devices is an efficient dissipation of seismic energy or introduction of additional damping. This should ensure adequate conditions for the control of intensive vibrations during very strong earthquake events.

To satisfy all the above stated conditions and specific requirements, a specific experimental large-scale bridge model was designed and built. The designed and constructed USI-SF bridge model is shown in Figure 5, Figure 18, and Figure 19.

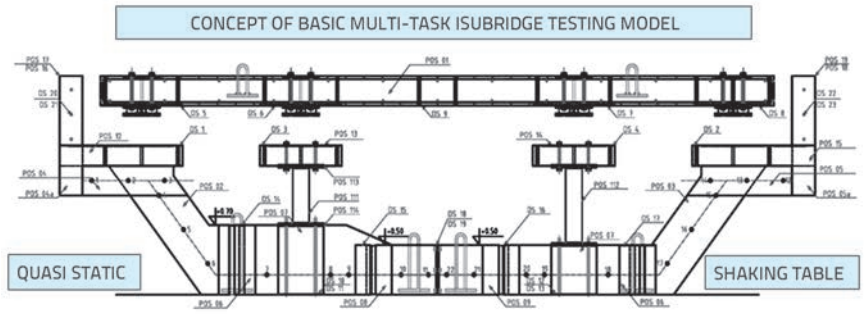

Figure 18. Designed principal multi-purpose bridge prototype model

Figure 19. USI-SF bridge prototype model for seismic behaviour testing installed on IZIIS seismic shaking table including two original SF-ED-4C-L1R-T1 devices and four DSRSB devices

a) Characteristics of bridge model substructure. The substructure of the experimental model of the prototype bridge is composed of two parallel rigid RC beams with the corresponding inclination at both ends to provide an elevated horizontal position for abutment supports. The horizontal parts of both parallel RC beams are used to enable suitable positioning of the bridge model on the seismic shaking table in the direction of its diagonal. The total length of horizontal part of RC beams is l_1 = 520.0 cm. The plan-view length of both ends with their extensions amounts to: l_2(left) = l_2(right) = 155.0 cm. With these dimensions, the total length of the substructure amounts to L_{DS} = 520.0 + 2 · 155.0 = 830.0 cm.

The two parallel beams are constructed to have a cross-section of b/h = 25 cm/50 cm. However, on the left side, the height of the cross-section is increased for 20.0 cm, amounting to b/h = 25/70 cm. In this way, the condition for building central piers with different heights has been fulfilled. Both parallel RC beams are mutually connected by six transverse RC beams, three on each half. The proportions of transverse beams on the left half of the substructure are: (1) b/h = 40/70 cm; (2) b/h = 50/70 cm and (3) b/h = 40/50 cm. The central transverse beam of the left half (b/h = 50/70 cm) is intended to be used as fixing support of the shorter piers, constructed as a pair of piers of steel material with a hollow circular cross-section. Proportions of transverse connecting beams on the right half are: (1) b/h = 40/50 cm; (2) b/h = 50/50 cm and (3) b/h = 40/50 cm. The middle transverse connecting beam (b/h = 50/50 cm) of this half is used to fix the bottom end of the longer piers constructed as a pair of piers of steel material with hollow circular cross-section. The inclined parts of parallel RC beams end with horizontal parts that are connected, at their very ends, with transverse RC beams and monolith cast-in place RC plates 20 cm in thickness. Both RC end slabs are used to install the left and right DSRSB devices and SF-ED devices between them, respectively, Figure 20 and Figure 23. Two vertical RC columns with cross-section a/b = 25/35 cm and a height of h = 70.0 cm are designed at each end of the bridge model RC substructure. These short columns assume the role of safety elements that support devices that are to control large displacements. The central piers are constructed in pairs of two steel piers, with a hollow circular cross-section 168 mm in diameter and 12.0 mm in wall thickness.

Figure 20. Constructed and installed set of two DSRSB devices and one SF-ED-4C-L1R-T1 device at right end support of the tested bridge prototype model

On the upper surface, the steel piers have end steel connecting plates that support RC bent slabs measuring 90 cm x 150 cm x 20 cm. Two positions for optional installation of a pair of DSRSB

devices, and SF-ED devices in the middle between them, are provided on the RC bent slabs.
The entire substructure is precast and composed of two parts of identical length (Figure 19 and Figure 22). The connection of these two parts is realized separately on two longitudinal RC beams in the middle by using front steel plates and the corresponding bolts. The prefabrication of the substructure is dependent on laboratory conditions, including the bearing capacity of the laboratory crane, limited to max Q = 100 kN.

b) Characteristics of bridge model superstructure. The superstructure of the model of the prototype bridge is constructed in form of a RC deck of required weight (Figure 18). To provide the necessary weight, the RC plate is constructed with the cross-section measuring b/d = 150/30 cm. The total length of the RC deck is l = 740.0 cm. A free space of $D_1 = D_2 = 20$ cm is left at each end. The width of the end vertical columns amounts to $b_1 = b_2 = 25.0$ cm. Again, considering these dimension at the top level, the total length of the entire experimental bridge model is L = 740.0 cm + 2 · 20.0 cm + 2 · 25.0 cm = 830.0 cm. The RC deck is placed at a height distance of $h_d = 40.0$ cm from the highest RC substructure surfaces. This space (seismic gap) is used for the location of two (2) metal spacers at each supporting position out of the four available ones (two end and two middle supporting positions). DSRSB devices are mounted on these metal spacers, while a space for installation of novel SF-ED devices is provided between the metal spacers, Figure 20.

c) Displacement limiting devices. A displacements limitation system (DLS) was designed and implemented to eliminate any risk from drop-down of the installed heavy bridge model superstructure during its strong dynamic response, and to ensure full test safety in the case of simulated very strong earthquakes, Figure 5. The present DL system consisted of 8 specific, so called displacement limiting devices (DLD) in the form of short flexible steel cantilevers, acting as nonlinear stoppers capable of avoiding dangerous "hard impact". This enables efficient functioning of the seismic isolation system composed of four DSRSB devices and energy dissipation system composed of two SF-ED devices, (Figure 23) since DL devices were placed at an equal safety distance providing gap of Dg = 60.0mm. These devices can be activated only in the case of excessive displacements and, in such cases, they provide restoring force capable of eliminating the risk of complete superstructure displacement during an experimental shaking table test.

6.2. Instrumentation of USI-SF bridge prototype model

An appropriate model instrumentation was applied to enable acquisition of representative experimental results during seismic testing of the assembled USI-SF bridge prototype model. It consisted of three different types of purpose-made instruments (sensors) (Figure 21), as follows:

a) LVDT transducers for relative displacement measurements. These transducers were used for measuring time histories of relative displacements between the substructure and superstructure of the bridge model. The main objective of these measurements was to define history of activation of DSRSB and SF-ED devices, since they react according to magnitude of relative displacements. A total of four LVDT type transducers were used for that purpose.

b) LP transducers for absolute displacement measurements. These transducers were used to record the time history of total displacement at selected characteristic points of the bridge

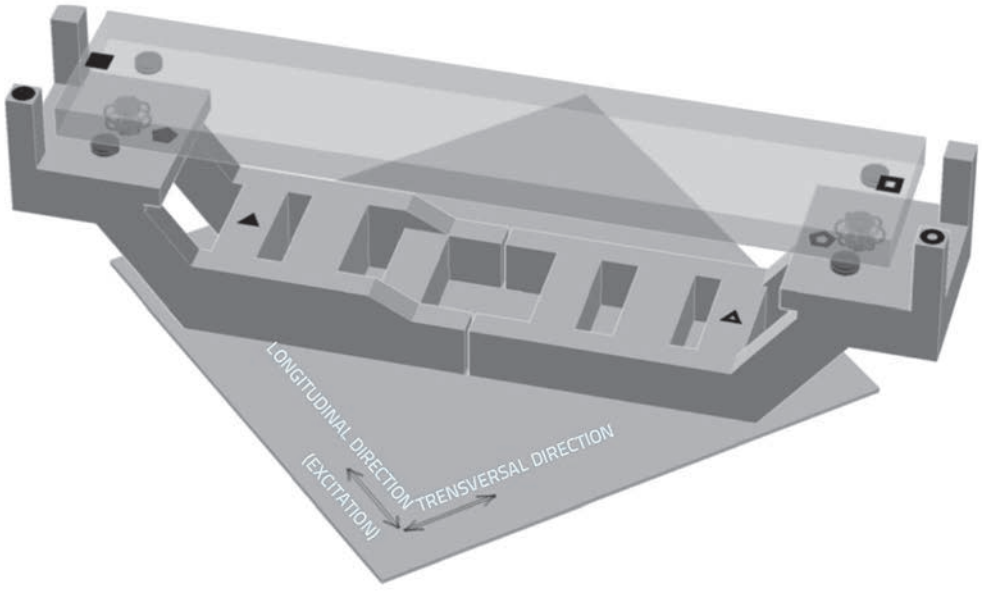

CH 01	NP1		L	LVDT-01
CH 02	NP1		T	LVDT-02
CH 03	NP2		L	LVDT-03
CH 04	NP2		T	LVDT-04
CH 05	NP3		L	LP-01
CH 06	NP4		L	LP-02
CH 07	NP7		L	LP-03
CH 08	NP8		L	LP-04
CH 09	NP3		L	ACC-01
CH 10	NP3		T	ACC-02
CH 11	NP4		L	ACC-03
CH 12	NP4		T	ACC-04
CH 13	NP5		L	ACC-05
CH 14	NP5		T	ACC-06
CH 15	NP6		L	ACC-07
CH 16	NP6		T	ACC-08
CH 17	NP7		L	ACC-09
CH 18	NP7		T	ACC-10
CH 19	NP8		L	ACC-11
CH 20	NP8		T	ACC-12

Figure 21. Acquisition points and sensors with respective recording channels

model. The total displacements are measured by fixing one end of the transducer directly onto the bridge model experiencing motion, while the other end is fixed to a respective reference point at the same height, located at the steel column located beyond the seismic shaking table (fixed to laboratory floor), which does not experience any displacement. Actually, the first two channels were used to record the motion of the substructure (LP-01 and LP-02), while the other two channels were used to record the motion of the superstructure (LP-03 and LP-04).

Figure 22. Laboratory assembly of large-scale USI-SF bridge prototype model on seismic shaking table for seismic testing under simulated real earthquakes

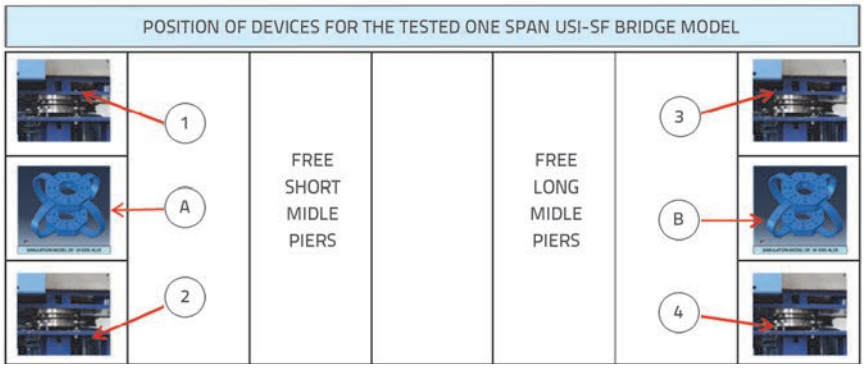

Figure 23. Positions of DSRSB devices (1 to 4) and SF-ED devices (A and B) of the tested one-span large-scale USI-SF bridge prototype model on seismic shaking table

c) ACC accelerometers for recording acceleration. These accelerometers were used to record the time histories of acceleration at selected characteristic points on the model of the bridge structure. Actually, six characteristic measuring points were selected and two acceleration components were measured at each point. The total of twelve channels were used to record acceleration time histories, as follows:

- *Channels for recording superstructure acceleration.* The bridge superstructure consists of a rigid RC deck. Therefore, two measuring points (one at each end) were selected, or four channels in total were used (channel 1 to channel 4);
- *Channels for recording acceleration in the upper zone of substructure.* Two measuring points were selected in the upper zone of the bridge model substructure. They were located on top of short RC piers on the left and the right side. Four channels (channel 5 to 8) were used for measuring two acceleration components at each point;
- *Channels for recording acceleration in the lower zone of substructure.* Two measuring points, located on the left and the right side of the base RC beam fixed to the seismic shaking table, were selected to get an insight into histories of acceleration in the lower zone of the bridge substructure. Four channels (channel 9 to channel 12) were used for measuring two acceleration components at each point.

6.3. Earthquake simulation for shaking table tests

After fabrication of model segments and specific SI, ED and DL devices, and after preparation of other testing connections and instrumentation devices, the large-scale USI-SF bridge prototype model was assembled on the seismic shaking table for the planned seismic testing under simulated real earthquake conditions. The assembly was done by transferring and installing constituent components in the laboratory of the Institute of Earthquake Engineering and Engineering Seismology (IZIIS) in Skopje (Figure 22 and Figure 19). After full instrumentation of the USI-SF bridge prototype model in compliance with the instrumentation programme, the representative seismic input and testing procedure was determined so as to enable generation of original test data as needed for this study.

The selection of representative seismic excitations has been done following IZIIS experience in simulating dynamic conditions that are as close as possible to the expected critical input for the considered real traditional non-isolated prototype bridge of this type, having fundamental period of about T≈0.5 sec. With the isolation system adopted in this study, the fundamental period of the selected prototype bridge was enlarged and amounted to T1 = 1.5 sec. Then the resulting real size isolated bridge system was considered as actual prototype for construction of a large-scale shaking table test model. Considering the present bridge model and other records, the following two recorded real earthquakes were selected as the representative seismic input:

- the earthquake record obtained during the El Centro earthquake (1940) in USA
- the earthquake record obtained during the Montenegro (1979) earthquake at the locality of Petrovac, both presented in Figure 24 and Figure 26.

To bring the frequency content of the selected earthquakes in accordance with dynamic characteristics of the scaled experimental model, the earthquake records were compressed by a time factor of FT = $1/\sqrt{R}$, where R = 9 represents geometrical scale of the bridge model. Both computed compressed earthquake records are presented as plots in Figure 25 and Figure 27, respectively.

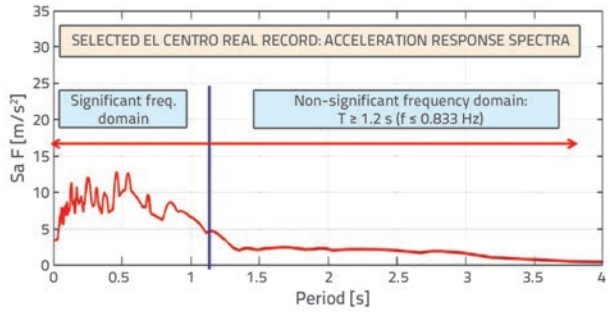

Figure 24. Acceleration response spectra of real (not time compressed) El Centro record representing actual frequency content

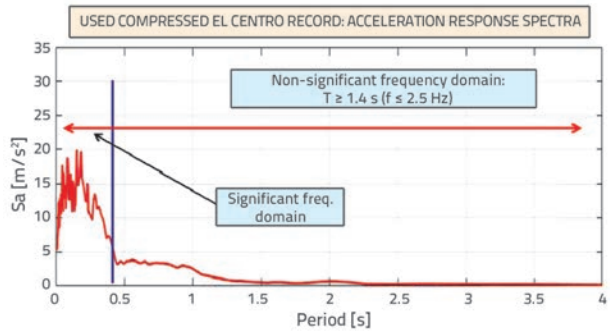

Figure 25. Acceleration response spectra of scaled time compressed El Centro record (PGA = 0.544g) with frequency content for testing

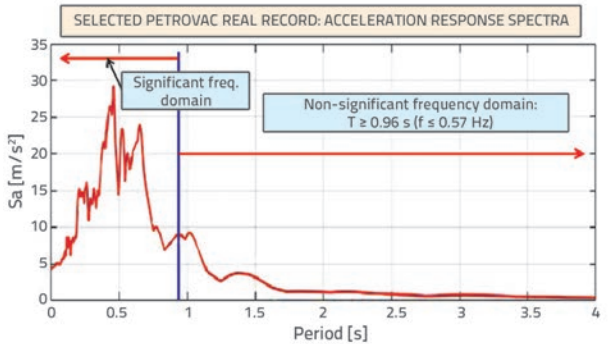

Figure 26. Acceleration response spectra of real (not time compressed) Petrovac record representing actual frequency content

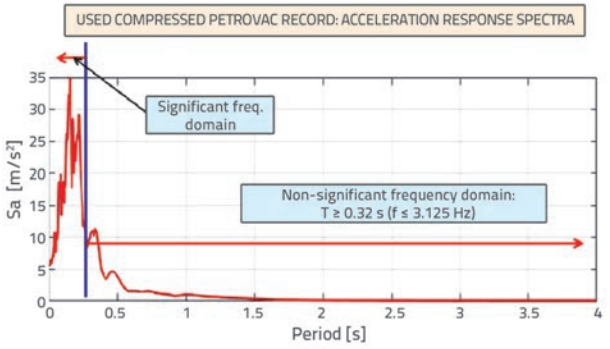

Figure 27. Acceleration response spectra of time compressed Petrovac record (PGA = 0.544g) with frequency content for testing

In order to gain the clearest possible insight into seismic performance of the advanced USI-SF system, very high intensities of shaking table input earthquakes were intentionally selected. The seismic shaking table tests of the USI-SF innovative system for seismic protection of bridge structures are highly valuable for answering many important questions. More precisely, it is necessary to see, based on this innovative system, the response for a built bridge being struck by an excessively strong earthquake and immediately after being struck by an earthquake, which will be as strong as the first one on the same location of the bridge. In that case, it would be possible to conclude whether the applied system for seismic protection possesses the capacity for successful protection of the bridge structure under repeated strong seismic effects. Due to high importance of the above issue, special attention was paid to this important aspect during experimental research. Actually, because of these reasons, the experimental procedure was devised so as to enable realization of the following three main steps:

- use the constructed multi-purpose bridge model and compose the advanced USI-SF bridge model by applying respective SI, ED and DL devices (Figure 23)
- perform the seismic shaking table tests (original and repeated) of USI-SF bridge model under simulated characteristic high-intensity earthquake
- process experimental results enabling quantification of real seismic performances of USI-SF bridge system and estimation of its suitability for practical application.

To obtain the experimentally confirmed answer to the questions about the system's capability to withstand repeated strong earthquakes, the implemented experimental procedure was realized in two steps. In step 1, the original shaking table test was performed using the assembled USI-SF bridge model 1. In step 2, the same tested model of a bridge was used once again and it "experienced the effect of a very strong earthquake" as model 2, and the shaking table test was repeated. Therefore, the experimental model 2 is marked as the USI-SF-R model, where R stands for repeated seismic tests. With realization of the full testing programme, including realization of four shaking table tests under strong earthquakes, it became possible to evaluate actual response characteristics of the studied USI-SF system and to estimate its practical applicability for an improved seismic protection of bridges.

6.4. Selected results from shaking table tests under original and repeated El Centro earthquake

Before seismic testing of the USI-SF model on the seismic shaking table, several sine-sweep tests were made to define damping and resonant frequencies of the constructed large-scale bridge model. However, a specific phenomenon was observed during initial shaking table tests realized by application of very low sine-sweep signals. Namely, the double spherical rolling seismic isolation system manifested a kind of an aperiodic behaviour for the acceleration input of A ≤ 0.01g since, in such case, the response

spectra do not exhibit pronounced resonance frequencies. Such behaviour is probably due to very small rolling amplitudes of balls when the curved surface shows an insignificant effect. Further on, sine-sweep tests were realized by simulating a stronger constant acceleration shaking table input with two intensity levels, A1 = 0.02g and A2 = 0.05g, considering a quite large frequency range of f = 1-35 Hz. The two fundamental mode shapes represent relative translation in x and y directions of the bridge model superstructure compared to the stiff model substructure.

The fundamental vibration period of T = 0.53s (f = 1.887 Hz) was defined for the case of the assembled bridge model involving installation of DSRSB devices only. However, the fundamental period of T = 0.35 s (f = 2.857 Hz) was obtained for the assembled complete bridge model, involving installation

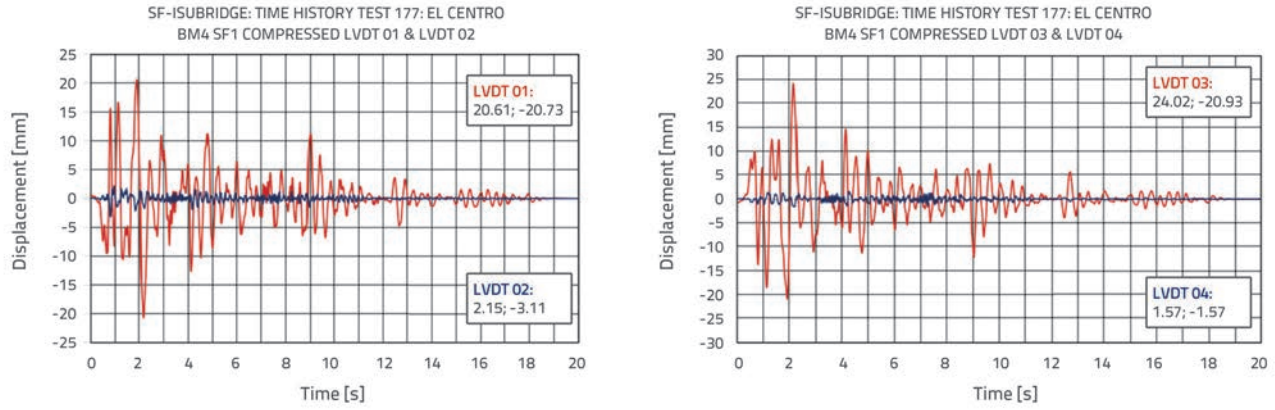

Figure 28. Original test-1 of USI-SF bridge model: Displacement recorded by LVDT01, 02, 03 & 04 under simulated El-Centro earthquake scaled to PGA = 0.77g on seismic shaking table

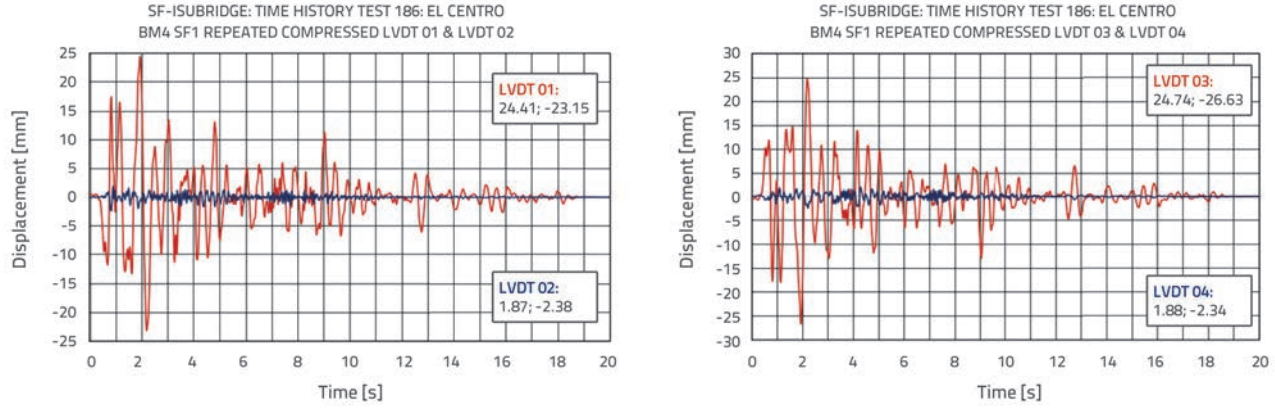

Figure 29. Repeated test-2 of USI-SF bridge model: Displacement recorded by LVDT 01, 02, 03 & 04 under simulated El-Centro earthquake scaled to PGA = 0.77g on seismic shaking table

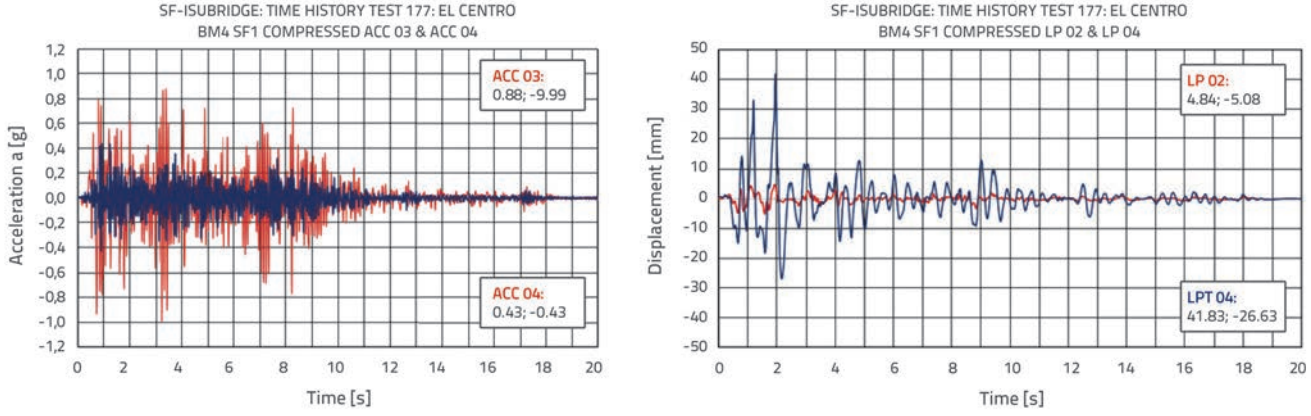

Figure 30. Original test-1 of USI-SF bridge model: Recorded acceleration by ACC 03&04 and absolute displacement by LP 02&04 under El-Centro earthquake scaled to PGA = 0.77g

of DSRSB & SF devices. The damping range ξ = 3.0-3.5% was defined for the case of the assembled complete model.
A large set of original experimental data was successfully recorded during first two shaking table tests of USI-SF bridge prototype model conducted with the simulated effect of time-compressed El Centro earthquake. However, only the most characteristic results - clearly demonstrating seismic response characteristics of the USI-SF bridge system - are presented in this study.

Very critical scenarios characterized by repeated strong ground shaking, or time extended strong earthquake excitations, were intentionally created via the test programs. Characteristic experimental results are presented in form of recorded time history functions of respective physical quantities in a representative set of figures, Figure 28, Figure 29, and Figure 30. In addition, the positive and negative peak values of physical quantities recorded successfully from all instrumentation

Table 2. Positive and negative relative substructure-superstructure peak displacements recorded by four LVDT sensors during original and repeated shaking table tests under El-Centro earthquake record

No.	Original seismic test-1 El-Centro earthquake PGA = 0.77 g			Repeated seismic test-2 El-Centro earthquake PGA = 0.77 g		
	Channel	MaxD (+) [mm]	MaxD (-) [mm]	Kanal	MaxD (+) [mm]	MaxD (-) [mm]
1	LVDT-01	20.61	20.73	LVDT-01	24.41	23.15
2	LVDT-02	2.15	3.11	LVDT-02	1.87	2.38
3	LVDT-03	24.02	20.93	LVDT-03	24.74	26.63
4	LVDT-04	1.57	1.57	LVDT-04	1.88	2.34

Table 3. Positive and negative absolute peak displacements recorded by four LP sensors during original and repeated shaking table tests under simulated compressed El-Centro earthquake record

No.	Original seismic test-1 El-Centro earthquake PGA = 0.77 g			Repeated seismic test-2 El-Centro earthquake PGA = 0.77 g		
	Channel	MaxD (+) [mm]	MaxD (-) [mm]	Kanal	MaxD (+) [mm]	MaxD (-) [mm]
1	LP-01	8.98	9.61	LP-01	9.13	9.30
2	LP-02	4.83	5.04	LP-02	4.89	5.07
3	LP-03	30.66	25.83	LP-03	34.70	27.30
4	LP-04	41.79	26.78	LP-04	41.47	29.15

Table 4. Positive and negative peak accelerations recorded by twelve ACC sensors during original and repeated shaking table tests under simulated compressed El-Centro earthquake record

No.	Original seismic test-1 El-Centro earthquake PGA = 0.77 g					Repeated seismic test-2 El-Centro earthquake PGA = 0.77 g				
	Channel	MaxA G (+)	DAF	MaxA G (-)	DAF	Kanal	MaxA G (+)	DAF	MaxA G (-)	DAF
1	ACC-01	0.40	0.52	0.45	0.58	ACC-01	0.33	0.42	0.43	0.56
2	ACC-02	0.17	0.22	0.17	0.22	ACC-02	0.17	0.22	0.15	0.19
3	ACC-03	0.88	1.14	0.99	1.28	ACC-03	1.13	1.47	1.13	1.47
4	ACC-04	0.44	0.57	0.43	o.56	ACC-04	0.55	0.71	0.46	0.60
5	ACC-05	0.38	0.49	0.33	0.42	ACC-05	0.37	0.48	0.35	0.45
6	ACC-06	0.15	0.19	0.16	0.20	ACC-06	0.19	0.25	0.17	0.22
7	ACC-07	0.66	0.85	0.55	0.71	ACC-07	0.82	1.06	0.91	1.18
8	ACC-08	0.71	0.92	0.60	0.78	ACC-08	0.69	0.90	0.62	0.80
9	ACC-09	0.73	o.95	0.68	0.88	ACC-09	0.70	0.91	0.68	0.88
10	ACC-10	0.14	0.18	0.14	0.18	ACC-10	0.19	0.25	0.17	0.22
11	ACC-11	0.63	0.82	0.61	0.79	ACC-11	0.60	0.78	0.59	0.77
12	ACC-12	0.13	0.17	0.11	0.14	ACC-12	0.13	0.17	0.12	0.15

channels are obtained and consistently summarized in respective tables (Table 2, Table 3, and Table 4). Each experimental acquisition channel recorded a large file with 120 000 numerical values. Twenty active channels were used for a single experimental test. Considering simultaneous recording with 20 active and some accessory channels, approximately 5.000.000 numerical values were recorded from only one experimental shaking table test of the USI-SF system performed on the IZIIS' seismic shaking table. The stated indicators clearly point out the importance of recorded original experimental data for validation of seismic performance of the USI-SF system under a very strong repeated El Centro earthquake.

Figure 28 and Figure 29 present time histories of relative displacements recorded with LVDT-01 up to LVDT-04 during the shaking table original test-1 and repeated test-2 of the USI-SF bridge model under the simulated compressed El-Centro earthquake scaled to PGA = 0.77g. The following observations can be made based on results presented in Figure 28 and Figure 29:

- the displacements recorded by LVDT-01 and LVDT-03 in the direction of earthquake excitation (L) are dominant during the total test time
- the displacements recorded by LVDT-02 and LVDT-04 in the direction normal to the earthquake excitation (T) are quite small and insignificant, showing realistic response in expected range
- Nearly the same maximum displacement amplitudes are recorded on both, the left and the right end of the superstructure, which is realistic and expected
- the seismic response of the USI-SF system is very similar in case of the original shaking table test-1 (Figure 28) and repeated shaking table test-2 (Figure 29), characterized with maxD = 24.02 mm and maxD = 26.63 mm, Table 2.

The last observation confirmed very stable behaviour of the USI-SF system for the effect of a very strong repeated earthquake. Acceleration time histories recorded at right superstructure end by ACC-03 (L-direction) and ACC-04 (T-direction) during the original shaking table test-1 of USI-SF bridge model under simulated compressed El-Centro earthquake scaled to PGA = 0.77g, are comparatively presented in Figure 30 (left). All other recorded acceleration histories are in very good correlation, confirming successful accomplishment of the full testing procedure. Table 4 shows positive and negative peak absolute accelerations recorded by 12 acceleration sensors at the selected substructure and superstructure recording points during original and repeated shaking table tests. The following main observations can be derived from the presented results:

- the acceleration histories recorded at superstructure points in the direction of earthquake excitation (ACC-03) are dominant during the total test time
- the accelerations recorded at substructure points as well as in the direction normal to the earthquake excitation (ACC-02) are much smaller, showing response in an expected range
- as expected, nearly the same maximum acceleration amplitudes were recorded on both, the left and the right end of the superstructure
- the seismic response of the USI-SF system is very similar in the case of original shaking table test-1 and repeated shaking table test-2 characterized with recorded maxA = 0.99G and maxA = 1.13G, respectively (Table 4).

The stable behaviour of the USI-SF system was thus confirmed once again. In the same table, DAF (dynamic amplification factor) directly demonstrates the relation between the response peak acceleration and the input peak acceleration (DAF = Ar/PGA) for all recording points and respective directions. The absolute displacement histories recorded in the L-direction by sensor LP-02 (substructure) and LP-04 (superstructure) during original shaking table test-1 of the USI-SF bridge model under compressed El-Centro earthquake scaled to PGA = 0.77g, are comparatively presented in Figure 30 (right). Positive and negative peak absolute displacements recorded by LP-sensors are presented in Table 3. The following observations can be made based on the results presented in this study:

- absolute displacements histories at superstructure points (LP-3 and LP-4) are dominant
- absolute displacements at substructure points (LP-1 and LP-2) are much smaller, showing response in the expected range
- maximum amplitudes recorded at the left and right superstructure ends are nearly the same (as expected)
- the seismic response of USI-SF system is very similar in the case of original and repeated shaking table test (Table 3) confirmed by recorded maxDabs = 41.79 mm and maxDabs = 41.47 mm, respectively.

6.5. Selected shaking table test results for original and repeated Petrovac earthquake

The original test-1 and repeated test-2 of bridge model present in a similar way seismic response characteristics of USI-SF bridge system under the effect of the strong Petrovac earthquake. The selected experimental results are comparatively presented in form of analogous time history plots in the set of figures, Figure 31, Figure 32, and Figure 33. Positive and negative peak values recorded by all instrumentation channels are consistently presented in respective tables, Table 5, Table 6, and Table 7. Displacement histories recorded by LVDT-01 up to LVDT-04 during original and repeated shaking table tests of the USI-SF bridge model under the compressed Petrovac earthquake scaled to PGA = 0.71g and PGA = 0.74g, are presented in Figure 31 and Figure 32, respectively. Similar observations can be made based on results obtained by these two tests:

- displacements recorded by LVDT-01 and LVDT-03 (L-direction) are dominant while displacements recorded by LVDT-02 and LVDT-04 (T-direction) are quite small and insignificant

- similar displacement amplitudes are recorded on both, the left and the right end of the superstructure, as expected
- seismic response of the USI-SF system is very similar in case of the original shaking table test-1 and repeated shaking table test-2 characterized with maxD = 19.21 mm and maxD = 18.96 mm (Table 5), showing once again a very stable behaviour of the USI-SF system for the effect of strong repeated earthquakes.

Acceleration histories recorded at the right superstructure end by ACC-03 (L-direction) and ACC-04 (T-direction) during the original shaking table test-1 of the USI-SF bridge model under the compressed Petrovac earthquake scaled to PGA = 0.71g, are comparatively presented in Figure 33 (left). Positive and negative absolute peak accelerations, recorded by acceleration sensors located at selected recording points

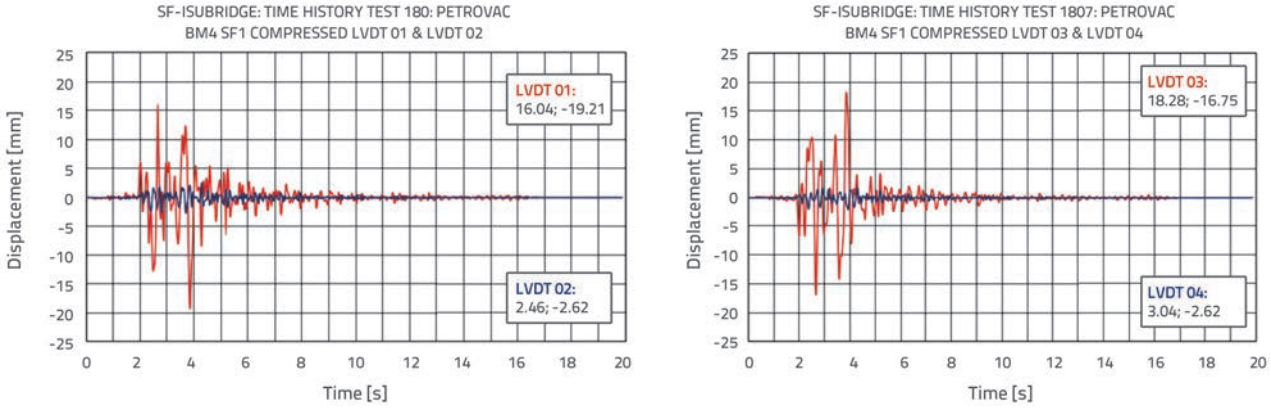

Figure 31. Original test-1 of USI-SF bridge model: Displacement recorded by LVDT'S 01, 02, 03 & 04 under simulated Petrovac earthquake scaled to PGA = 0.71g on seismic shaking table

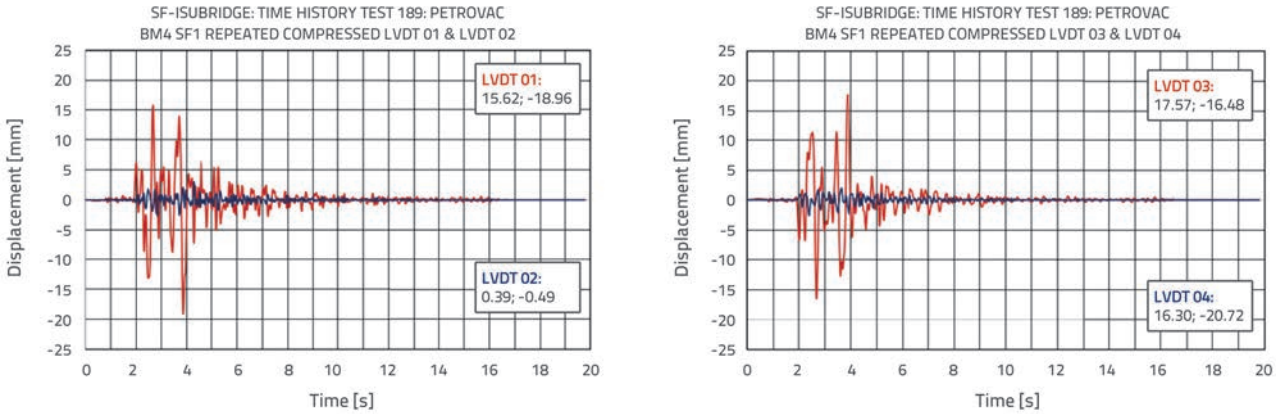

Figure 32. Repeated test-2 of USI-SF bridge model: Displacement recorded by LVDT'S 01, 02, 03 & 04 under simulated Petrovac earthquake scaled to PGA = 0.74g on seismic shaking table

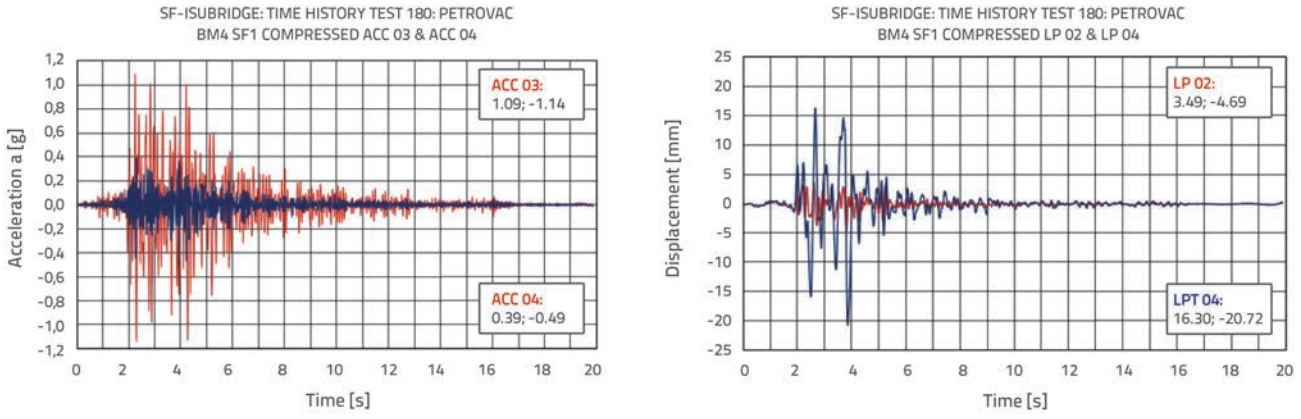

Figure 33. Original test-1 of USI-SF bridge model: Recorded acceleration by ACC'S 03&04 and absolute displacement by LP'S 02&04 under Petrovac earthquake scaled to PGA = 0.71g

during original and repeated shaking table tests, are given in Table 7. Comparison of the original and repeated shaking table test shows that the seismic response of the USI-SF system is very similar, characterized with recorded maxA = 1.14g and maxA = 1.25g, respectively (Table 7). The presented DAF factors demonstrate similar response and input relations. Absolute displacements recorded in the L-direction LP-02 (substructure) and LP-04 (superstructure) direction during the original shaking table test-1 of the USI-SF bridge model are presented in Figure 33 (right). Positive and negative absolute peak displacements recorded by four LP-sensors are presented in Table 6. Seismic response of the USI-SF system was very similar in case of original and repeated test (Table 6), confirming once again reliable behaviour of novel USI-SF system under strong repeated earthquakes.

Table 5. Positive and negative relative substructure-superstructure peak displacements recorded by four LVDT sensors during original and repeated shaking table tests under Petrovac earthquake

No.	Original seismic test-1 Petrovac earthquake PGA = 0.71 g			Repeated seismic test-2 Petrovac earthquake PGA = 0.74 g		
	Channel	MaxD (+) [mm]	MaxD (-) [mm]	Kanal	MaxD (+) [mm]	MaxD (-) [mm]
1	LVDT-01	16.04	19.21	LVDT-01	15.62	18.96
2	LVDT-02	2.46	2.62	LVDT-02	3.04	2.62
3	LVDT-03	18.28	16.75	LVDT-03	17.57	16.48
4	LVDT-04	1.67	1.96	LVDT-04	2.10	2.60

Table 6. Positive and negative peak displacements recorded by four LP sensors during original and repeated shaking table tests under simulated compressed Petrovac earthquake record

No.	Original seismic test-1 Petrovac earthquake PGA = 0.71 g			Repeated seismic test-2 Petrovac earthquake PGA = 0.74 g		
	Channel	MaxD (+) [mm]	MaxD (-) [mm]	Kanal	MaxD (+) [mm]	MaxD (-) [mm]
1	LP-01	6.46	6.61	LP-01	6.30	6.62
2	LP-02	3.49	4.69	LP-02	3.45	4.89
3	LP-03	15.35	18.39	LP-03	16.67	17.67
4	LP-04	16.30	20.72	LP-04	15.94	19.85

Table 7 Positive and negative peak accelerations recorded by twelve ACC sensors during original and repeated shaking table tests under simulated compressed Petrovac earthquake record

No.	Original seismic test-1 Petrovac earthquake PGA = 0.71 g					Repeated seismic test-2 Petrovac earthquake PGA = 0.74 g				
	Channel	MaxA G (+)	DAF	MaxA G (-)	DAF	Kanal	MaxA G (+)	DAF	MaxA G (-)	DAF
1	ACC-01	0.42	0.59	0.41	0.58	ACC-01	0.38	0.51	0.41	0.55
2	ACC-02	0.20	0.28	0.19	0.25	ACC-02	0.18	0.24	0.15	0.20
3	ACC-03	1.09	1.41	1.14	1.60	ACC-03	1.10	1.49	1.25	1.69
4	ACC-04	0.39	0.51	0.49	0.64	ACC-04	0.41	0.55	0.50	0.67
5	ACC-05	0.28	0.39	0.34	0.48	ACC-05	0.27	0.36	0.30	0.40
6	ACC-06	0.23	0.30	0.24	0.31	ACC-06	0.21	0.28	0.26	0.35
7	ACC-07	0.70	0.98	0.83	1.08	ACC-07	0.65	0.88	0.82	1.11
8	ACC-08	0.42	0.54	0.53	0.69	ACC-08	0.48	0.65	0.54	0.73
9	ACC-09	0.70	0.98	0.70	0.98	ACC-09	0.72	0.97	0.71	0.96
10	ACC-10	0.15	0.21	0.20	0.28	ACC-10	0.16	0.22	0.21	0.28
11	ACC-11	0.64	0.83	0.59	0.83	ACC-11	0.65	0.88	0.60	0.81
12	ACC-12	0.13	0.18	0.11	0.15	ACC-12	0.13	0.17	0.11	0.15

6.6. Main observations from shaking table tests

The following observations can be made based on integral results of the shaking table model tests of the novel USI-SF bridge system: (1) the DSRSB devices represent an excellent option for seismic isolation of bridge superstructure as they provide large and safe displacement capacity in all directions; (2) the SF-ED devices represent an advanced option for seismic energy dissipation providing large displacement capacity with very stable hysteretic behaviour in all directions for an imposed deep response nonlinearity; (3) the proposed USI-SF bridge system represents a favourable innovative general option for seismic protection of bridge structures under very strong earthquakes; (4) the integral advanced USI-SF bridge system exhibits high capacity to sustain cyclic multi-peak deep nonlinear response; (5) after experiencing the effect of very strong earthquakes, the system will not experience any significant damage; (6) the system generally possesses confirmed capability to function successfully under repeated seismic effects without conducting any interventions to repair or change the devices, and (7) the system showed capability to remain in operation without considerable effects to its normal functioning. Consequently, the above stated observations represent a direct experimental confirmation of the advanced seismic performances of the integral USI-SF system, important for successful achievement of a qualitatively improved seismic protection of bridges under very strong repeated earthquakes.

7. Conclusions

The following general conclusions can be made based on research results obtained through extensive experimental and theoretical studies, using the innovative USI-SF bridge model prototype: (1) The optimized novel DSRSB seismic isolators are highly attractive and effective passive devices for seismic isolation of bridges in arbitrary direction. However, for their application on any particular bridge, seismic isolators should be designed based on advanced integrated response modification concept and analysis procedures; (2) The advanced multi-directional hysteretic SF energy dissipation devices possess unique energy absorption features, since they are capable of adapting stable behaviour to the actual arbitrary earthquake direction, as well as to the actual intensity of the seismic input energy. In fact, the advanced SF-ED devices provide innovative, very stable and advanced 3D hysteretic response in the most critical cases of repeated strong earthquake effects in all directions; (3) The displacement limiting devices, DLD, represent a very effective obligatory measure and the last line of defence from excessive displacement of bridge superstructure. It is clear that the installed displacement limiting devices represent an efficient passive system providing additional contribution to the improvement of the bridge seismic safety and are activated only in critical cases involving very strong earthquakes; (4) Experimental tests made in this study confirm that the advanced USI-SF system potentially represents an upgraded high-performance seismic isolation option for bridges. The system is based on an optimized seismic energy balance, and represents an effective complete technical innovation capable of integrating the advantages of seismic isolation, seismic energy dissipation, and effective displacement control. The developed and tested USI-SF system shows very high seismic response modification performances and could be used for efficient seismic protection of bridges in all directions under the effect of very strong repeated earthquakes; and (5) In further studies, creative analytical research activities should be performed, and a particular emphasis should be placed on the development of generalized practical design rules of the developed advanced USI-SF system for seismic protection of various representative types of highway bridges, designed with different structural, material and geometrical properties, and subjected to repeated earthquakes with different intensities and frequency content.

Acknowledgements

This extensive experimental and analytical research was realized at IZIIS, University "SS Cyril & Methodius", Skopje, in the scope of the three year innovative NATO Science For Peace and Security Project: *Seismic Upgrading of Bridges in South-East Europe by Innovative Technologies (SFP: 983828), with participation of five countries: Macedonia: D. Ristic, Leader & PPD-Director, Germany: U. Dorka, NPD-Director, Albania: A. Lako, Bosnia & Herzegovina: D. Zenunovic & Serbia: R. Folic.* Creation of RESIN Laboratory, as a new open testing lab of the Regional Seismic Innovation Network involving young scientists, was an accepted long-term specific task. A comprehensive NATO support in the realization of the integral long-term and costly innovative research project is highly appreciated.

REFERENCES

[1] Kelly, J.M.: Aseismic base isolation: A review and bibliography, Soil Dynamics and Earthquake Engineering, 5 (1986), pp. 202-216.

[2] Kunde, M.C., Jangid, R.S.: Seismic behaviour of isolated bridges: A-state-of-the-art review, EJSE, Electronic Journal of Structural Engineering, 3 (2003).

[3] Turkington, D.H., Carr, A.J., Cooke, N., Moss, P.J.: Seismic design of bridges on Lead-rubber bearings, Journal of Structural Engineering, ASCE, 115 (1989) a, pp. 3000-3016.

[4] Robinson, W.H.: Lead-rubber hysteretic bearings suitable for protecting structures during earthquakes, Earthquake Engineering and Structural Dynamics, 10 (1982), pp. 593-604.

[5] Dolce, M., Cardone, D., Palermo, G.: Seismic isolation of bridges using isolation systems based on flat sliding bearings, Bulletin of Earthquake Engineering, 5 (2007) 4, pp. 491–509.

[6] Iemura, H., Taghikhany, T., Jain, S.K.: Optimum Design of Resilient Sliding Isolation System for Seismic Protection of Equipments, Bulletin of Earthquake Engineering, 5 (2007) 1, pp. 85–103.

[7] Kartoum, A., Constantinou, M.C., Reinhorn, A.M.: Sliding isolation system for bridges: Analytical study, Earthquake Spectra, 8 (1992), pp. 345-372.

[8] Wang, Y.P., Chung, L., Wei, H.L.: Seismic response analysis of bridges isolated with friction pendulum bearings, Earthquake Engineering and Structural Dynamics, 27 (1998).

[9] Zayas, V.A., Low, S.S. and Mahin, S.A.: A simple pendulum technique for achieving seismic isolation, Earthquake Spectra, 6 (1990), pp. 317-334.

[10] Mokha, A., Constantinou, M.C., Reinhorn, A.M.: Teflon bearings in seismic base isolation I: Testing, Journal of Structural Engineering, ASCE, 116 (1990), pp. 438-454.

[11] Constantinou, M.C., Kartoum, A., Reinhorn, A.M., Bradford, P.: Sliding isolation system for bridges: Experimental study, Earthquake Spectra, 8 (1992), pp. 321-344.

[12] Skinner, R.I., Kelly, J.M., Heine, A.J.: Hysteretic Dampers for earthquake resistant structures, Earthquake Engineering and Structural Dynamics, 3 (1975), pp. 287-296.

[13] Guan, Z., Li, J., Xu, Y.: Performance Test of Energy Dissipation Bearing and Its Application in Seismic Control of a Long-Span Bridge, Journal of Bridge Engineering, ASCE, 2010.

[14] Tsopelas, P., Constantinou, M.C., Kim, Y.S., Okamoto, S.: Experimental study of FPS system in bridge seismic isolation, Earthquake Engineering and Structural Dynamics, 25 (1996) a, pp. 65-78.

[15] Jankowski, R., Wilde, K., Fujino, Y.: Pounding of superstructure segments in isolated elevated bridge during earthquakes, Earthquake Eng. and Struct. Dynamics, 27 (1998), pp. 487-502.

[16] Tubaldi, E., Mitoulis, S. A., Ahmadi, H., Muhr, A.: A parametric study on the axial behaviour of elastomeric isolators in multi-span bridges subjected to horizontal seismic excitations, Bulletin of Earthquake Engineering, 14 (2016) 4, pp. 1285-1310.

[17] Serino, G., Occhiuzzi, A.: A semi-active oleodynamic damper for earthquake control: Part 1: Design, manufacturing and experimental analysis of the device, Bulletin of Earthquake Engineering, 1 (2003) 2, pp. 269-301.

[18] Mayes, R.L, Buckle, I.G., Kelly, T.E., Jones, L.R.: AASHTO Seismic isolation design requirements for highway bridges, Journal of Structural Engineering, ASCE, 118 (1992), pp. 284-304.

[19] Unjoh, S., Ohsumi, M.: Earthquake response characteristics of super-multispan continuous menshin (seismic isolation) bridges and the seismic design, ISET Journal of Earthquake Engineering Technology, 35 (1998), pp. 95-104.

[20] Dolce, M., Filardi, B., Marnetto, R., Nigro, D.: Experimental tests and applications of a advanced biaxial elastoplastic device for the passive control of structures, Proc. of 4th World congress on joint sealants and bearing systems for concrete structures, Sacramento, California (USA), 1996.

[21] Ene, D., Yamada, S., Jiao, Y., Kishiki, S., Konishi. Y.: Reliability of U-shaped steel dampers used in base-isolated structures subjected to biaxial excitation, Earthquake Engineering & Structural Dynamics, 46 (2017) 4, pp. 621–639.

[22] Oh, S.H., Song, S.H., Lee, S.H., Kim, H.J.: Seismic response of base isolating systems with U-shaped hysteretic dampers, Int. Journal of Steel Structures, 12 (2012) 2, pp 285–298.

[23] Candeias, P., Costa, A.C., Coelho, E.: Shaking table tests of 1:3 reduced scale models of four story unreinforced masonry buildings, 13th World Conf. on Earthquake Eng., Vancouver, Paper: 2199, 2004.

[24] Ristic, D., Ristik, J.: Advanced Integrated 2G3 Response Modification Method for Seismic Upgrading of Advanced and Existing Bridges, 15th World Conference on Earthquake Engineering, (WCEE), Lisbon, Portugal, 2012.

[25] Ristic, D.: Nonlinear Behaviour and Stress-Strain Based Modeling of Reinforced Concrete Structures Under Earthquake Induced Bending and Varying Axial Loads, Doctoral Dissertation, School of Civil Engineering, Kyoto University, Kyoto, Japan, 1988.

[26] Ristik, J.: Comparative Seismic Analysis of RC Bridge Structure Applying Macedonian Seismic Design Regulations and Eurocodes, MSc Thesis, Department for Theory of Structures, University SS Cyril and Methodius, Skopje, Macedonia, 2011.

[27] Ristik, J.: Modern Technology for Seismic Protection of Bridge Structures Applying Advanced System for Modification of Earthquake Response, PhD Thesis, Institute of Earthquake Engineering and Engineering Seismology (IZIIS), University SS Cyril and Methodius, Skopje, Macedonia, 2016.

[28] Wilson, L.E.: Three-Dimensional Static and Dynamic Analysis of Structures: A Physical Approach With Emphasis on Earthquake Engineering, Berkeley, California: Third Ed., 2002.

[29] Bathe, K.J.: Finite element procedures in engineering analysis, Prentice-Hall, 1982.

[30] Zienkiewicz, O.C., Taylor, R.: The Finite Element Method – Volume 1: The Basis, Fifth Edition, Berkeley, California, 2000.

[31] Chopra, K.A.: Dynamics of Structures. Theory and Applications to Earthquake Eng., Berkeley, 1995.

[32] Clough, R.W., Penzien, J.: Dynamics of Structures, McGraw-Hill, Advanced York, N.Y., 1975.

[33] Kelly, J.M., Dimitrios, A.K.: Mechanics of Rubber Bearings for Seismic and Vibration Isolation, John Wiley & Sons, 2011.

[34] Priestley, M.J.N., Seible, F., Calvi, G.M.: Seismic Design and Retrofit of Bridges, John Wiley & Sons, Advanced York, 1996.

[35] Wilson, E.L., Habibullah A.: SAP2000, Structural and earthquake engineering software, Computers and Structures Inc., Berkeley, California, USA.

[36] ABAQUS: Software for finite element analysis and computer-aided engineering, ABAQUS Inc., USA.

[37] ANSYS Mechanical: Finite element analysis (FEA) software, ANSYS, Inc., USA.